EYAS JAMAL ABU-RADDAD

The Pharmacokinetics, Stereoselectivity and Allometric Scaling of Fluorinated Cytosine Analogues

(Under the direction of F. DOUGLAS BOUDINOT)

The pharmacokinetics of a hypothetical prodrug of a cytosine analogue, and the stereoselective and allometric scaling of the pharmacokinetics of a cytidine analogue are investigated. Flucytosine (5-fluorocytosine, 5-FC) has been used for decades to treat systemic fungal infections, but its use was limited by serious side effects at high plasma concentrations. The azido-pyrimidine, 4-azido-5-fluoro-2(1H)-pyrimidinone (A-5-FP) has been synthesized as a potential prodrug for 5-FC in an attempt to dampen high concentrations encountered with 5-FC administration. 2',3'-Dideoxy-5-fluoro-3'-thiacytidine (RCV; Racivir™), is a chiral compound whose enantiomers are potent inhibitors of human immunodeficiency virus (HIV) and hepatitis B virus (HBV).

A-5-FP did not convert to 5-FC after intravenous administration, suggesting the absence of enzymes necessary to reduce the azide group into amine functionality. A-5-FP distributed slower to a similar apparent volume, and was cleared faster than 5-FC.

The stereoselective pharmacokinetics of RCV was fully characterized in rats. Chiral inversion was not observed *in vivo*. Differences in plasma profiles between the two enantiomers were not readily visible. Nonetheless, the (+)-enantiomer had higher renal and nonrenal clearances, central and steady-state distribution volumes, and apparent absorption rate and extent. A weak enantiomeric interaction was detected, reducing steady-state distribution volume and slowing the absorption of both enantiomers.

Nonlinear mixed effects modeling (NONMEM) was used to characterize allometric relationships describing differences in the disposition of the (−)-enantiomer of RCV, namely (−)-FTC, between 4 animal species. The initial model was deficient and mispredicted pharmacokinetic profiles and parameters in all species. When lower than expected clearance of (−)-FTC, and higher adipose tissue fraction in woodchuck were accounted for, predictions were enhanced appreciably. The estimates of allometric

exponents for clearances and volumes were closely in agreement and not significantly different from the theoretical values of ¾ for functional properties like clearances, and 1 for structural properties like volumes. The model predicted the pharmacokinetic properties for a 70-kg man to be 27.7 and 21.5 L/h for total and distributional clearances, and 40.3 and 32.8 L for central and peripheral volumes, respectively. The accuracy of such predictions remains to be verified.

INDEX WORDS: Anti-viral, Anti-fungal, 5-Fluorocytosine, 4-Azido-5-fluoro-2(1H)-pyrimidinone, Racivir™, RCV, FTC, HIV, HBV, Stereoselective pharmacokinetics, NONMEM, Mixed effects, Allometric scaling.

THE PHARMACOKINETICS, STEREOSELECTIVITY AND ALLOMETRIC SCALING OF FLUORINATED CYTOSINE ANALOGUES

by

EYAS JAMAL ABU-RADDAD

B.S., The University of Jordan, Jordan, 1997

A Dissertation Submitted to the Graduate Faculty of The University of Georgia in Partial Fulfillment of the Requirements for the Degree

DOCTOR OF PHILOSOPHY

ATHENS, GEORGIA

2001

THE PHARMACOKINETICS, STEREOSELECTIVITY AND ALLOMETRIC SCALING OF FLUORINATED CYTOSINE ANALOGUES

by

EYAS JAMAL ABU-RADDAD

Approved:

Major Professor: F. Douglas Boudinot

Committee: Anthony C. Capomacchia
Daniel B. Hall
D. Robert Lu
James T. Stewart

Electronic Version Approved:

Gordhan L. Patel
Dean of the Graduate School
The University of Georgia
December 2001

From whom I descend, Huda and Jamal,

and to whom I belong, Laith, Jana, Sara’ and Ahmad,

with love.

ACKNOWLEDGEMENTS

The words are frail when I express my appreciation to Dr. F. D. Boudinot. I was heartened by the support, patience, guidance, and sensitivity he provided me with during my various endeavors and hardships in the past few years.

I would like to thank Drs. Daniel B. Hall and James T. Stewart for their scholarly competent help they continuously supplied. My thanks extend to Drs. Anthony C. Capomacchia and D. Robert Lu for their timely assistance and encouragement.

To the clan of Barrow Hall, the ones who are still here, and the ones whose presence is still felt, I give my thanks for continuous encouragement and companionship, and for making my years at the University of Georgia pleasant and enjoyable.

I would also like to express my deep appreciation to the encouragement I received from my friends wherever they are. I especially acknowledge the unrelenting support in time of need Mohannad continually provided.

TABLE OF CONTENTS

CHAPTER 1

INTRODUCTION AND LITERATURE REVIEW

Nucleic bases and their corresponding nucleosides and nucleotides are the basic blocks of the genetic material of all living matter on which the function and propagation of both host and invading organisms depend. Mimicking naturally occurring components of genetic material has been exploited to halt or slow the progression of undesired growth of internal or external origins. Such conditions include human immunodeficiency virus (HIV), hepatitis B virus (HBV), and systemic fungal infections, as well as malignancies.

The epidemic of the acquired immunodeficiency syndrome (AIDS) is a paradigm for emerging infectious diseases of the modern medical era. Initially recognized in a small number of men in a few cities in the United States, the number of persons with human immunodeficiency virus (HIV) infection and AIDS grew rapidly around the world, and is now a major pandemic affecting almost every inhabited part of the world. The AIDS syndrome is characterized by sever immunosuppression, opportunistic infections, and cancers that result from infection with HIV.[1]

The management of AIDS has advanced dramatically, from diagnosing and treating associated late opportunistic infections to the use of potent and effective antiretroviral therapies. HIV reverse transcriptase (HIV-RT) and aspartyl proteases are the main targets for antiretroviral action. HIV-RT is responsible for the conversion of the single stranded RNA chain into a double stranded DNA chain, and aspartyl protease is an essential enzyme for the production of viral structural proteins that are capable of being assembled into infectious viral particles.[1,2]

The most important therapeutic strategy for the therapy of HIV infection at the current time is the use of highly active antiretroviral therapy (HAART). HAART

combines a protease inhibitor and two nucleoside analogues as HIV-RT inhibitors, or alternatively, two nucleoside analogues combined with a nonnucleoside reverse transcriptase inhibitor.[3] Although potent, antiretroviral agents have been inadequate in eradicating the virus from sanctuary tissues in the body, like the lymph nodes and brain.[4] Combined with serious side effects associated with available anti-HIV therapy, this fact makes the development of new antiretroviral agents an imperative.

More than 1 billion people have been infected with and 300 million people are chronic carriers of HBV. Chronic carriers are exposed to a high risk of mortality due to developing cirrhosis and hepatocellular carcinoma. Despite the availability of efficient vaccines, HBV infection remains a major public health problem worldwide. Only few options are present for the treatment of HBV infections, and are limited by low efficacy, relapse or dose-dependent side effects. The development of new antiviral agents remains of high importance.[5]

HBV virus uses a polymerase, similar to retroviral reverse transcriptase that has multiple functions including signals for viral pregenome encapsidation, priming of reverse transcription, RNA dependent-DNA synthesis, DNA dependent-DNA synthesis, and RNase-H activity. It is therefore an ideal target for antiviral compounds.[6]

Systemic mycoses are emerging as life-threatening conditions, and their incidence continues to rise. This increase is due in part to improved recognition and diagnosis of fungal infections, but also to the prolonged survival of immunocompromised patients like cancer and AIDS patients. Cryptococcus and Candidia, among other fungi, infect various organs in the body, most commonly the brain, lungs and kidneys.[7]

Many analogues of nucleic bases and nucleosides have been developed and/or approved for HIV, HBV and systemic fungal infections. A few nucleoside analogues have been approved by the United States Food and Drug Administration (FDA) for the treatment of HIV infection, including zidovudine (AZT), didanosine (ddI), zalcitabine (ddC), stavudine (d4T), lamivudine (3TC) and abacavir sulfate (1592U89). Lamivudine

was the first and only nucleoside analogue to be approved for the treatment of chronic HBV infections. However, many nucleoside analogues have been investigated or are currently being investigated as anti-HBV agents. The list includes adenine arabinoside (araA, Vidarabine); acyclic nucleoside analogues like acyclovir, ganciclovir, and penciclovir; and dideoxycytidine analogues like 2',3'-dideoxy-5-fluoro-3'-thiacytidine, a compound closely related to lamivudine.[8] Flucytosine (5-fluorocytosine, 5-FC) has been in use for systemic candida and cryptococcal infections for decades.

Nucleoside analogues exert their action by the conversion to their corresponding triphosphates by cellular kinases that act on the naturally occurring nucleosides, followed by the inhibition of HIV-RT and HBV-polymerase, or the incorporation into the growing viral DNA resulting in DNA chain termination.[9,10] 5-FC is converted intracellularly to 5-fluorouracil (5-FU), which is in turn phosphorylated and incorporated in RNA to alter protein synthesis, or interrupt DNA synthesis by inhibiting thymidylate synthetase.[11]

A brief description of an analogue of cytosine and another of cytidine follows, namely 4-azido-5-fluoro-2(1H)-pyrimidinone (A-5-FP), a hypothetical prodrug of 5-FC, and 2',3'-dideoxy-5-fluoro-3'-thiacytidine (RCV).

4-Azido-5-fluoro-2(1H)-pyrimidinone (A-5-FP)

The use of 5-FC is limited by bone marrow and liver toxicities encountered at high concentrations.[12] In an effort to overcome the toxicity of 5-FC at high concentrations, a prodrug might offer a dampening effect on the higher concentrations, and prolong the half-life of the drug.

Nucleoside analogues where an azide group was introduced have been used as prodrugs for their amine counterparts. Azido-purine prodrugs of the nucleosides 2'-F-ara-ddA and ara-A have been shown to convert to their amino-counterparts in vivo.[13,14] Similarly, 4-azido-5-fluoro-2(1H)-pyrimidinone (A-5-FP) has been synthesized as a potential prodrug for 5-FC. It is hypothesized that a reductase enzyme system analogous

to the reductase acting on the azido-purine analogues would catalyze the conversion of the azido-pyrimidine A-5-FP to 5-FC.

2′,3′-Dideoxy-5-fluoro-3′-thiacytidine (RCV)

Additional pharmacotherapies for the treatment of hepatitis B virus (HBV) and human immunodeficiency virus (HIV) infections with improved pharmacological and toxicological profiles are needed.[15] Among the most potent compounds are 2′,3′-dideoxycytidine analogs, such as 2′,3′-dideoxy-3′-thiacytidine (BCH-189) and 2′,3′-dideoxy-5-fluoro-3′-thiacytidine (RCV, Racivir™), which have shown high activity against HIV and HBV.[16-21] In general, the S-(−) enantiomers of BCH-189 and RCV, lamivudine (3TC; Epivir®) and emtricitabine ((−)-FTC; Coviracil®), corresponding to the unnatural L form, possess greater antiviral activity in cultured cells[16,18,20,22-25] than the corresponding R-(+) enantiomers.[18,20,23,24]

RCV structure possesses two chiral centers, one of which is enantiomerically pure as the R configuration at 4′ position, and the other, at 1′ position, exists as R and S configurations, corresponding to the enantiomers R-(+)- and S-(−)-FTC, respectively (Figure 3-1). The pharmacokinetics of RCV and (−)-FTC have been investigated in mice,[26] rats,[27,28] cynomolgus monkeys,[26] woodchucks,[29,30] and rhesus monkeys.[31] Meanwhile, since stereoselective assay for the determination of (+)- and (−)-FTC in biological matrices has not yet been reported, the potential chiral inversion and enantiomeric interactions of FTC have not been addressed to date.

Stereoselectivity in drug development

The pharmacokinetics of new chemical entities forms the basis for understanding the dose-concentration-effect relationships, and designing dosing regimens. Hence, the absorption, distribution, metabolism and elimination of drug candidates are investigated early in the drug development process. Compounds with favorable pharmacokinetic

profiles constitute more attractive candidates because of improved compliance through less frequent administration via a convenient route of administration.

Asymmetry of drug molecules is an interesting and challenging feature in drug development. Stereoisomers are molecules having the same structural formulas but differ from each other only in the way the atoms or groups are oriented in space. Stereoisomers whose mirror images are not superimposable due to asymmetry around a tetravalent carbon are called enantiomers. This property of nonsuperimposition is termed chirality and the subtructural feature that gives rise to this asymmetry is called the chiral center. Enantiomers are optically active molecules that have identical chemical and physical properties, and differ only in the direction of the rotation of plane-polarized light. The 50:50 mixture of two enantiomers is called a racemic mixture.[32]

Due to the inherent chirality of biological media, it is reasonable to expect that enantiomers of chiral molecules could exhibit differences in the disposition and action. Bodies comprised of macromolecules that consist of chiral building blocks see the racemic mixture not as a single compound, but as a mixture of two distinct molecules with different pharmacological activities, toxicities, and dispositional properties.[33,34]

Differences between enantiomers can be further complicated by the administration of racemic mixtures. The presence of one enantiomer can affect the properties of the antipode in the mixture. This interaction between enantiomers, can affect absorption, distribution, metabolism or elimination of one of or both enantiomers.[35,36] Pharmacodynamics may also be affected. One enantiomer might be a competitive inhibitor of the other by having affinity to the receptor, without having intrinsic activity.[37,38]

In addition, the stereoselective inversion of one enantiomer to the other *in vivo* has been documented. This phenomenon is particularly marked in the series of 2-arylpropionic acid type non-steroidal anti-inflammatory analgesics related to ibuprofen[39] This was also reported for stiripentol, a new antiepileptic agent.[40] With this in mind, it is

readily realized that pharmacokinetic studies conducted using non-stereoselective analytical method can be misleading.

Regulatory bodies, including the United States Food and Drug Administration (FDA), have set guidances for the development of chiral compounds after thoughtful discussions and symposia about this matter. The general consensus was that when a practical and economically viable route to the enantiomer with the desired activity can be established on a production scale, this should be the preferred form of the drug for development. Use of the racemate, it was argued, ought to be viewed as polytherapy and treated accordingly. This does not rule out the development of racemic mixtures, but highly encourages the development of pure enantiomers. It was also emphasized that an enantiospecific analytical methodology should be implemented in studies involving enantiomers. Conditions like chiral inversion and enantiomer-enantiomer interactions could only be discerned by the use of such methods.[41,42] An increasing wealth of such techniques have been recently developed, utilizing high performance liquid chromatography (HPLC), gas chromatography (GC) and capillary electrophoresis (CE), among others.[43]

Physiology, anatomy, pharmacokinetics and body size

Animals have been used in early development to gain knowledge about the action and fate of new chemical entities. In this context, animals are used as surrogates for humans to minimize loss or injury of human souls. Nevertheless, differences between animal models and humans in action, metabolism and disposition of xenobiotics exist. If the differences remained unexplained, the use of animals can only be regarded as a proof of the concept of activity or a media for comparison between different chemical entities.

Scaling relationships have been a persistent theme in biology at least since the time of Leonardo da Vinci and Galileo.[44] The most promising theory of body size and metabolic rate is that which integrates the considerations on heat exchange and

circulation. In natural selection, those animals probably prove to be the fittest whose cells are adapted to a level of oxygen consumption at which the overall metabolic rate is suitable for the maintenance of a constant body temperature and commensurate with an efficient transport of oxygen.[45]

The largest, most complex organisms, large mammals and giant trees, weigh more than 21 orders of magnitude more than the simplest microbes, yet they use basically the same molecular structures and biochemical pathways to sustain and reproduce themselves. It follows that biological diversity is largely a matter of size, and organisms must adjust their structure and function to compensate for the geometric, physical, and biological consequences of being different sizes, maintaining self-similarity. Such self-similarity is said to be fractal that can be described by a fractal dimension or a power function.[44]

The concept portrayed above is fairly new,[46] but the use of power functions to characterize scaling laws has a much longer history. Power laws have long been used in biology to relate body size, surrogated by weight (W), to structural and functional properties (Y). These laws are known as allometric equations, and take the form of

$$Y = a\, W^{b} \tag{1-1}$$

where a and b are the allometric coefficient (the property value at unit body weight) and exponent, respectively.[47] It follows that the relationship between $log(Y)$ and $log(W)$ is linear with a slope of b, and an intercept of $log(a)$.The geometric scaling of linear dimensions as a function of volume (size) of a self-similar geometric object is a familiar example of allometry. Geometry scales to the power of multiples of a third. However, organisms do not usually exhibit such simple geometric scaling. This is because there are powerful constraints on structure and function that do not allow organisms to maintain the same geometric relationships among their components as size changes over several

orders of magnitude.[44] It was empirically found that many physiological and anatomical properties of mammals, and most living organisms for this matter, scale to multiples of ¼, known as the quarter-power-law. Biological times usually scale to the power of ¼, volumes to the power of 1, and functions like flows and metabolic rates to the power of ¾. Multiple attempts to explain such phenomena have been suggested,[47] but until recently, none has been supported by a solid theory, and there remains a tendency to treat scaling relationships as purely empirical phenomena.[44] The books of Peters,[47] McMahon and Bonner[48] and Bonner, Schmidt-Nielson,[49] and Calder[50] in the early eighties summarized accumulated work on allometry.[44]

It was not until 1997 that the empiricism of allometry was augmented by a solid theory that not only furnished a theoretical explanation of the allometric relationship of mammalian physiological and anatomical properties, but also extended them to other organisms, including other nonmammalian animals, plants and insects. A mechanism and a general model were set forth to account for quarter-power scaling in biology.[51] The idea is that biological rates and times are ultimately limited by the rates at which energy and materials can be distributed between surfaces where they are exchanged and the tissues where they are used. The model assumes that the distribution network branches to reach all parts of a three-dimensional organism, has terminal units that do not vary with size, and minimizes the total resistance and hence the energy required to distribute resources. It predicts that the network will have a fractal-like architecture, that many anatomical and physiological features will scale as quarter powers of body mass, and that the whole-organism metabolic rate should scale to body weight raised to the power of ¾. The acceptance of this model as a general explanation for the origin of scaling laws in biology is yet to be assessed, and deviations from the quarter-power law need to be addressed.[44]

Pharmacokinetic properties of xenobiotics can also be scaled to body weight using the allometric relationship. The underlying premise is that pharmacokinetic

properties, as distribution volumes and clearances, are dependent on or correlate with allometrically scalable anatomical structures or physiological processes, like organ or fluid volumes, metabolizing organs blood flow, and glomerular filtration rate. The metabolism of alcohol was the first example of a scaled pharmacokinetic parameter.[52] Ever since, many attempts have been made to explain pharmacokinetic differences between mammals on the basis of body weight.

The impetus for the use of allometry in pharmacokinetics is to be able to predict pharmacokinetic properties of new chemical entities in man prior to the administration of first human dose. Allometry may suggest a more reasonable starting dose for dose ranging phase-I clinical trials, and offers to reduce the range of doses, time, or number of studies needed, with subsequent reduction in overall drug development time and expense.

Most published allometric practices are retrospective in nature, with a reporting bias for examples where the prediction of already known pharmacokinetic properties in man is successful. Failure of allometric scaling to predict drug fate in man is rarely reported, and therefore, the logical and useful application of allometric scaling as a prospective predictive tool is yet to be explored. Recently, Bonate and Howard critiqued the prospective potential of allometric scaling. Their premise was that prediction intervals are too large to be useful, and that it is not possible to determine which drugs will fail a priori. They suggest reporting instances in which prospective allometric scaling has failed so that scientists may begin to see the factors of success or failure with better prediction of human pharmacokinetics.[53]

Pahlman et al[54] and Lave et al[55] have shown that drugs that are secreted in the bile may not be predicted by currently known allometric approaches. Mahmood[56] has shown that total, as well as renal clearance, of renally secreted drugs may not be predicted with accuracy. In general, allometric scaling of clearance works best for renally excreted and rapidly metabolized compounds, when elimination is dependent on physiological parameters, like glomerular filtration rate and renal or hepatic blood flow,

which themselves scale allometrically.[57] For metabolized compounds with low to intermediate extraction ratios, reliable estimates of clearance can be obtained when allometric scaling is combined with in-vitro data.[58] In addition, species differences in plasma protein binding can affect the scalability of pharmacokinetic properties.[59]

It could be argued that the success of the allometric approach in predicting human pharmacokinetics, and its use in guiding the first human dose should be carefully implemented. Integrating the available data for a new chemical entity (preclinical pharmacokinetics, pharmacodynamic and toxicity) with data from other compounds in the same pharmacological class, and compounds with similar dispositional properties, can enhance the odds for success. At Hoffman La Roche, such integration has lead to a rational selection of the starting dose in humans, which was always higher than the dose predicted from toxicity data, yet safely administered.[60]

In forthcoming studies, the preclinical pharmacokinetics of A-5-FP and 5-FC are evaluated in rats, with the possibility of conversion of A-5-FP to 5-FC. The pharmacokinetics of the enantiomers of RCV, namely (+)-FTC and (−)-FTC are also fully characterized and compared, including possible chiral inversion and enantiomer-enantiomer interactions, following intravenous and oral administration of RCV, (+)-FTC and (−)-FTC to rats. Data for (−)-FTC in rats is added to data collected in three other species, and an allometric relationship that explains interspecies differences in the pharmacokinetics of (−)-FTC is established. Species-specific information are accounted for and incorporated in such a relationship, and the premise that pharmacokinetic properties scale allometrically to exponents of ¾ and 1 for functions and volumes, respectively, is tested.

References

1. Wormser G. P. (Ed.). AIDS and other manifestations of HIV infection. 1998. Lippincott-Raven Publishers, Philadelphia, PA.
2. De Clercq, E. 1992. HIV inhibitors targeted at the reverse transcriptase. AIDS Res. Hum. Retroviruses. **8**:119-134.
3. Carpenter, C. C. J., M. A Fischl, S. M. Hammer. 1997. Antiretroviral therapy for HIV-1 infection in 1997. JAMA **277**:1962-1969.
4. Cavert, W., D. W. Notermans, K. Staskus, S. W. Wietgrefe, M. Zupancic, K. Gerhard, K. Henry, Z.-Q. Zhang, R. Mills, H. Mcdade, J. Goudsmit, S. A. Danner, and A. T. Haase. 1997. Kinetics of response in lymphoid tissues to antiretroviral therapy of HIV-1 infection. Science. **276**:960-964.
5. Lee, W. M. 1997. Hepatitis B virus infection. N. Engl. J. Med. **337**:1733-1745.
6. Seeger C., and W. S. Mason. 1993. Hepadnavirus replication and approaches to anticiral therapy. In: W. Doerfler, and P. Bohm (Eds.), Virus Strategies. Ch. 4. VCH, Germany. pp 77-93.
7. Perfect, J. R. Cryptococcosis. M. A. Crislip and J. E. Edwards, Jr. Candidiasis. 1989. In: Systemic fungal infections: Diagnosis and treatment. W. B. Saunders Company, Philadelphia, PA pp. 77-137.
8. Hong, J. H., Y. Choi, B. K. Chun, K. Lee, and C. K. Chu.1998. Current status of anti-HBV chemotherapy. Arch. Pharm. Res. **21**(2):89-105.
9. Dolin, R., H. Masur, and M. S. Saag. (Eds.) 1999. AIDS Therapy. Churchill Livingstone, Philadelphia, PA.
10. Zoulim, F. 1999. Therapy of chronic hepatitis B virus infection: inhibition of the viral polymerase and other antiviral strategies. Antiviral Research. **44**:1-30.
11. Bennet, J. E. 1977. Flucytosine. Annals of Internal Medicine. **86**:319-322.

12. Bennett J. E. 1990. Antifungal agents. In: Goodman and Gillman: The Pharmacological Basis of Therapeutics. McGraw-Hill, New York, NY. pp. 1168-1169.

13. Koudiakova, T., K. K. Manouilov, K. Shamuganathan, L. P. Kotra, F. D. Boudinot, E. Cretton-Scott, J. P. Sommadossi, R. F. Schinazi, and C. K. Chu. 1996. *In vitro* and *in vivo* evaluation of 6-azido-2',3'-dideoxy-2'-fluoro-β-D-arabinofuranosylpurine and N^6-methyl-2',3'-dideoxy-2'-fluoro-β-D-arabinofuranosyladenine as prodrugs of anti-HIV nucleosides 2'-F-ara-ddA and 2'-F-ara-ddI. J. Med. Chem. **39**:4676-4681.

14. Kotra, L. P., K. K. Manouilov, E. Cretton-Scott, J. P. Sommadossi, F. D. Boudinot, R. F. Schinazi, C. K. Chu. 1996. Synthesis, biotransformation, and pharmacokinetic studies of 9-(β-D-arabinofuranosyl)-6-azidopurine: A prodrug for ara-A designed to utilize the azide-reduction pathway. J. Med. Chem. **39**:5202-5207.

15. Schinazi R. F., J. R. Mead, P. M. Feorino. 1992. Insights into HIV chemotherapy. AIDS Res. Hum. Retroviruses **8:**963-990.

16. Chang C.-N., S.-L. Doong, J. H. Zhou, J. W. Beach, L. S. Jeong, C. K. Chu, C. Tsai, and Y.-C. Cheng. 1992. Deoxycytidine deaminase-resistant stereoisomer is the active form of (±)-2´,3´-dideoxy-3´-thiacytidine in the inhibition of hepatitis B virus replication. J. Biol. Chem. **267:**13938-13942.

17. Doong S.-L., C.-H. Tsai, R. F. Schinazi, D. C. Liotta, and Y.-C. Cheng. 1991. Inhibition of the replication of hepatitis B virus *in vitro* by 2´,3´-dideoxy-3´-thiacytidine and related analogues. Proc. Natl. Acad. Sci. USA **88:**8495-8499.

18. Schinazi R. F., C. K. Chu, A. Peck, A. McMillan, R. Mathis, D. Cannon, L. S. Jeong, J. W. Beach, W.-B. Choi, S. Yeola, and D. C. Liotta. 1992. Activities of the four optical isomers of 2´,3´-dideoxy-3´-thiacytidine (BCH-189) against human

immunodeficiency virus type 1 in human lymphocytes. Antimicrob. Agents Chemother. **36:**672-676.

19. Schinazi R. F., D. C. Liotta, W.-B. Choi, A. Peck, H. McClure, F. D. Boudinot, J.-P. Sommadossi, M. Davis, P. A. Furman, and G. Painter. 1992. Cellular pharmacology and monkey pharmacokinetics of the antiviral (−)-2′,3′-dideoxy-5-fluoro-3′-thiacytidine (FTC). National Collaborative Drug Discovery Group, Frontiers in HIV Therapy, San Diego, Calif., Nov. 3-7, p. 59.
20. Schinazi R. F., A. McMillan, D. Cannon, R. Mathis, R. M. Lloyd, A. Peck, J.-P. Sommadossi, M. St. Clair, J. Wilson, P. A. Furman, G. Painter, W.-B. Choi, and D. C. Liotta. 1992. Selective inhibition of human immunodeficiency viruses by racemates and enantiomers of *cis*-5-fluoro-1-[2-(hydroxymethyl)-1,3-oxathiolan-5-yl]cytosine. Antimicrob. Agents Chemother. **36:**2423-2431.
21. Soudeyns H., X.-J. Yao, Q. Gao, B. Belleau, J.L. Kraus, N. Nguyen-ba, B. Spira, and M. A. Wainberg. 1991. Anti-human immunodeficiency virus type 1 activity and in vitro toxicity of 2′-deoxy-3′-thiacytidine (BCH-189), a novel heterocyclic nucleoside analog. Antimicrob. Agents Chemother. **35:**1386-1390.
22. Cammack, N., P. Rouse, C. L. P. Marr, P. J. Reid, R. E. Boehme, A. V. Coates, C. R. Penn, and J. M. Cameron. 1992. Cellular metabolism of (−) enantiomeric 2′-deoxy-3′-thiacytidine. Biochem. Pharmacol. **43:**2059-2064.
23. Coates, J. A. V., N. Cammack, H. J. Jenkinson, I. M. Mutton, B. A. Pearson, R. Storer, J. M. Cameron, and C. R. Penn. 1992. The separated enantiomers of 2′-deoxy-3′-thiacytidine (BCH-189) both inhibit human immunodeficiency virus replication in vitro. Antimicrob. Agents Chemother. **36:**202-205.
24. Furman P. A., M. Davis, D. C. Liotta, M. Paff, L. W. Frick, D. J. Nelson, R. E. Dornsife, J. A. Wurster, L. J. Wilson, J. A. Fyfe, J. V. Tuttle, W. H. Miller, L. Condreay, D. R. Averett, R. F. Schinazi, and G. R. Painter. 1992. The anti-hepatitis B virus activities, cytotoxicities, and anabolic profiles of the (−) and (+)

enantiomers of *cis*-5-fluoro-1-[2-(hydroxymethyl)-1,3-oxathiolan-5-yl]cytosine. Antimicrob. Agents Chemother. **36:**2686-2692.

25. Mathez, D., R. F. Schinazi, D. C. Liotta, and J. Leibowitch. 1993. Infectious amplification of wild-type human immunodeficiency virus from patients' lymphocytes and modulation by reverse transcriptase inhibitors in vitro. Antimicrob. Agents Chemother. **37:**2206-2211.
26. Frick, L. W., C. U. Lambe, L. St. John, L. C. Taylor, and D. J. Nelson. 1994. Pharmacokinetics, oral bioavailability, and metabolism in mice and cynomolgus monkeys of (2´ *R*, 5´ *S*-)-*cis*-5-fluoro-1-[2-(hydroxymethyl)-1,3-oxathiolan-5-yl]cytosine, an agent active against human immunodeficiency virus and human hepatitis B virus. Antimicrob. Agents Chemother. **38**:2722-2729.
27. Abobo, C. V., L. Ni, R. F. Schinazi, D. C. Liotta, and F. D. Boudinot. 1994. Pharmacokinetics of 2´,3´-dideoxy-5-fluoro-3´-thiacytidine in rats. J. Pharm. Sci. **83**:96-99.
28. Frick, L. W., L. St. John, L. C. Taylor, G. R. Painter, P. A. Furman, D. C. Liotta, E. S. Furfine, and D. J. Nelson. 1993. Pharmacokinetics, oral bioavailability, and metabolic disposition in rats of (−)-*cis*-5-fluoro-1-[2-(hydroxymethyl)-1,3-oxathiolan-5-yl]cytosine, a nucleoside analog active against human immunodeficiency virus and hepatitis B virus. Antimicrob. Agents Chemother. **37:**2285-2292.
29. Cullen, J. M., S. L. Smith, M. G. Davis, S. E. Dunn, C. Botteron, A. Cecchi, D. Linsey, D. Linzey, L. Frick, M. T. Paff, A. Goulding, and K. Biron. 1997. In vivo antiviral activity and pharmacokinetics of *cis*-5-fluoro-1-[2-(hydroxymethyl)-1,3-oxathiolan-5-yl]cytosine in woodchuck hepatitis virus-infected woodchucks. Antimicrob. Agents Chemother. **41:**2076-2082.

30. Fox, L. M., M. A. Ascenzi, B. C. Tennant, J. Shi, R. F. Schinazi, and F. D. Boudinot. Stereoselective pharmacokinetics and metabolism of 2´-deoxy-5-fluoro-3´-thiacytidine (FTC) in woodchucks. Submitted for publication.

31. Schinazi, R. F., F. D. Boudinot, S. S. Ibrahim, C. Manning, H. M. McClure, and D. C. Liotta. 1992. Pharmacokinetics and metabolism of racemic 2´,3´-dideoxy-5-fluoro-3´-thiacytidine in rhesus monkeys. Antimicrob. Agents Chemother. **36**:2432-2438.

32. Aboul-Enein, H. Y., and L. I. Abou Basha. Chirality and drug hazards. In: H. Y. Aboul-Enein, and I. W. Wainer (Eds.). The Impact of Stereochemistry on Drug Development and Use. 1997. John Wiley & Sons, Inc., New York, NY.

33. Hubbard, J. W., D. Ganes, H. K. Lim, and K. K. Midha. 1986. Chiral pharmacology and its consequences for therapeutic monitoring. Clinical Biochemistry. **19**:107-112.

34. Williams, K. M. 1989. Chirality: Pharmacokinetics and pharmacodynamics in 3 dimensions. Clinical and Experimental Pharmacology and Physiology. **16**:465-470.

35. McGraw, N. P., P. S. Callery, N. Castagnoli Jr. 1977. Invitro stereoselective metabolism of the psychotromimetic amine 1-(2,5-dimethoxy-4-methylphenyl)-2-aminopropane. An apparent enantiomeric interaction. J. Med. Chem. 20:185-189.)(Lee E. J. D., K. Williams, R. Day, G. Graham, D. Champion. 1985. Stereoselective disposition of ibuprofen enantiomers in man. Br. J. Clin. Pharm. **19:**669-674.

36. Murphy, P. J, R. C. Nickander, G. M. Bellamy, and W. L. Kurtz. 1976. Effect of *l*-propoxyphene on plasma levels and analgesic activity of *d*-propoxyphene in the rat. J. Pharm. Exp. Ther. **199:**415-422.

37. Ariens, E. J. 1982. Stereochemistry, a basis for sophisticated nonsense in pharmacokinetics and clinical pharmacology. Eur. J. Clin. Pharmacol. 26:663-668.

38. Ariens, E. J. 1963. Steric structure and activity of catecholamines on alpha- and beta-receptors. In: K. L. Brunnings and P. Lindren (Eds.). Modern concepts in the relationship between structure and pharmacological activity, Vol. 7, pp. 247-264.

39. Hutt, A. J.,J. Caldwell. 1983. The metabolic chiral inversion of 2-arylpropionic acids—a novel route with pharmacological consequences. J. Pharm. Pharmacol. **35**:693-704.

40. Zhang, K., C. Tang, M. Rashed, D. Cui, F. Tombert, H. Botte, F. Lepage, R. H. Levy, and T. A. Baillie. 1994. Metabolic chiral inversion of stiripentol in the rat. I. Mechanistic studies. Drug Metab. Disp. **22**:544-553.

41. Baillie, T. A., and K. M. Schultz. Stereochemistry in the drug development process: Role of chirality as a determinant of drug action, metabolism, and toxicity. In: H. Y. Aboul-Enein, and I. W. Wainer (Eds.). The Impact of Stereochemistry on Drug Development and Use. 1997. John Wiley & Sons, Inc., New York, NY.

42. FDA's Policy Statement for The Development of New Stereoisomeric Drugs. 1992 Chirality **4**:338-340.

43. Ariens E. J., in A. M. Krstulovic (Editor), Chiral Separation by HPLC, Applications to Pharmaceutical Compounds, Ellis Horwood Limited, W. Sussex, England, 1989, p. 31.

44. Brown, J. H., and G. B. West. Scaling in Biology. 2000. Oxford University Press, New York, NY.

45. Kleiber, M. The Fire of Life: An introduction to animal energetics. Robert E. Krieger Publishing Co., Inc. 1975. pp. 200-201.

46. Mandelbrot, B. B. The Fractal Geometry of Nature. W. H. Freeman. New York, NY. 1983.

47. Peters, R. H. The Ecological Implications of Body Size. Cambridge University Press, New York, NY. 1983.

48. McMahon, T., and J. T. Bonner. On Size and Life. Scientific American Books, New York, NY. 1983.

49. Schmidt-Nielson, K. Scaling, Why Is Animal Size so Important?. Cambridge University Press, New York, NY. 1984.

50. Calder, W. A., III. Size, Function, and Life History. Harvard University Press, Cambridge, MA. 1984.

51. West, G. B., J. H. Brown, and B. J. Enquist. 1997. A general model for the origin of allometric scaling laws in biology. Science. **276**:122-126.

52. Lester, D., and W. Z. Keokosky. 1967. Alcohol metabolism in the horse. Life Sci. **6**:2313-2317.

53. Bonate, P. L., D. Howard. 2000. Critique of prospective allometric scaling: Does the emperor have clothes? J. Clin. Pharmacol. **40**:335-340

54. Pahlman, I., M. Edholm, S. Kahkaanranta, M.-L. Odell. 1998. Pharmacokinetics of susalimod, a highly biliary-excreted sulphasalazine analogue, in various species: nonpredictable human clearance by allometric scaling. J. Pharm. Pharmacol. **49**:494-498.

55. Lave, T. H., R. Portmann, G. Schenker, A. Gianni, A. Guenzi, M.-A. Girometta, M. Schmitt. 1999. Interspecies pharmacokinetic comparisons and allometric scaling of napsagatran, a low molecular weight thrombin inhibitor. J. Pharm. Pharmacol. **51**:85-91

56. Mahmood, I. 1998. Interspecies scaling of renally secreted drugs. Life Science. **63**:2365-2371.

57. Boxenbaum, B., R. W. D'Souza. 1990. Inter-species pharmacokinetic scaling, biological design and neoteny. In: Testa, B. (Ed.) Advances in Drug Research, Academic Press, London, p. 139-196.

58. Lave, T. H., R. Portmann, G. Schenker, A. Gianni, A. Guenzi, M.-A. Girometta, M. Schmitt. 1999. Interspecies pharmacokinetic comparisons and allometric scaling of napsagatran, a low molecular weight thrombin inhibitor. J. Pharm. Pharmacol. **51**:85-91

59. Mahmood, I. 2000. Interspecies scaling: role of protein binding in the prediction of clearance from animals to humans. J. Clin. Pharmacol. **40**(12) Pt 2:1439-1446.

60. Reigner, B. G., P. E. O. Williams, I. H. Patel, J.-L. Steimer, C. Peck, and P. V. Brummelen. 1997. An evaluation of the integration of pharmacokinetic and pharmacodynamic principles in clinical drug development. Clin. Pharmacokinet. **33**(2):142-152.

CHAPTER 2

PHARMACOKINETICS OF 4-AZIDO-5-FLUORO-2(1H)-PYRIMIDINONE AND 5-FLUOROCYTOSINE IN RATS[1]

---

[1]Eyas J. Abu-Raddad, Lakshmi P. Kotra, Chung K. Chu and F. Douglas Boudinot. Submitted to *Biopharmaceutics and Drug Disposition*.

Abstract

The use of flucytosine (5-FC), a fungistatic cytosine analogue, has been limited by life threatening bone marrow toxicity encountered at sustained high plasma levels of the drug. In an effort to reduce high levels of 5-FC and prolong its half-life, an azido-pyrimidine compound was synthesized by replacing the amine function in 5-FC with an azide group as a potential prodrug for 5-FC. 4-Azido-5-fluoro-2(1H)-pyrimidinone (A-5-FP) was designed to convert to 5-FC utilizing the P-450 reductase enzyme system that proved successful with azido-purine prodrugs. A reproducible, accurate and sensitive ion-pair HPLC method was developed to determine the concentration of 5-FC, A-5-FP and a potential metabolite 5-FU, simultaneously in plasma and urine. A-5-FP and 5-FC were administered intravenously to two groups of rats at equimolar doses of 60 and 50 mg/kg, respectively. Plasma samples over a 12-h period, and urine samples at 24 h were collected. Unlike the case with azido-purine prodrugs, A-5-FP did not convert to its amino counterpart, 5-FC. Volume of distribution at steady state was close to 1 L/kg for both 5-FC and A-5-FP indicating intracellular distribution and perhaps entrapment by cellular binding. Total body clearance was higher for A-5-FP, while distributional clearance was lower. Both renal and nonrenal clearances were higher for A-5-FP. Renal clearance for both 5-FC and A-5-FP, 0.48 L/h/kg and 1.74 L/h/kg, respectively, were greater than glomerular filtration rate in rats indicating active tubular secretion. Nonrenal clearance of 5-FC was low compared to A-5-FP, at 0.13 L/h/kg and 0.87 L/h/kg, respectively. These results suggest the absence of a specific azide-reduction pathway for azido-pyrimidine compounds in rats.

Introduction

Flucytosine (5-fluorocytosine, 5-FC), a fluorine analogue of cytosine (Figure 2-1), is a fungistatic agent that has been used in combination with amphotericin B for the treatment of systemic fungal infections including central nervous system cryptococcosis and candidiasis [1,2]. 5-FC is actively transported into cells by cytosine permease, and then it is converted to 5-fluorouracil (5-FU) by cytosine deaminase, an enzyme that is present in fungal but not mammalian cells (Figure 2-1). 5-FU can be converted to nucleotide anabolites by enzymes that normally act upon uracil. As much as 50% of the nucleotide is incorporated in RNA, resulting in alterations in protein synthesis [3, 4]. It was also found that interruption of DNA synthesis caused by the formation of 5-fluoro-2'-deoxyuridylic acid (FdUMP) with resultant inhibition of thymidylate synthetase is yet another mechanism of action [5].

Serious side effects of 5-FC, including bone marrow suppression and liver toxicity, are frequently encountered at serum concentration greater than 100 mg/L [6-8]. In an effort to overcome the toxicity of 5-FC at high concentrations, a prodrug might offer a dampening effect on the higher concentrations, and prolong the half-life of the drug. An azido-purine prodrug of the anti-HIV purine nucleoside 2'-F-ara-ddA, namely 6-azido-2',3'-dideoxy-2'-fluoro-β-D-arabinofuranosylpurine (FAAddP), was previously synthesized, and conversion to the parent drug was shown both in vitro and in vivo by the reduction of the azide group into an amine function, followed by deamination, yielding 2'-F-ara-ddI (Figure 2-2). The conversion of FAAddP to 2'-F-ara-ddA in mice was mediated by microsomal P-450 NADPH reductase system [9]. Similarly, the azide group in the prodrug 9-(β-D-arabinofuranosyl)-6-azidopurine (6-AAP), was converted to amine function by mouse cytochrome P-450 to yield 9-(β-D-arabinofuranosyl)adenine (ara-A), an anti Herpes simplex, antitumor agent (Figure 2-2). Administering 6-AAP prolonged the half-life of ara-A by 7-14 times compared with the administration of ara-A [10].

Applying the same concept, an azido-pyrimidine compound was synthesized, namely 4-azido-5-fluoro-2(1H)-pyrimidinone (A-5-FP), as a potential prodrug of 5-FC. So far, it has not been reported that an azide group in an azido-pyrimidine compound has shown conversion to an amine function. It is hypothesized that a reductase enzyme system analogous to the reductase acting on the azido-purine FAAddP and 6-AAP would catalyze the conversion of the azido-pyrimidine A-5-FP to 5-FC (Figure 2-1). The purpose of this report is to characterize the disposition of 5-FC and A-5-FP in rats, including possible conversion to 5-FC or 5-FU.

Materials and Methods

Chemicals. 4-Azido-5-fluoro-2(1H)-pyrimidinone (A-5-FP) was synthesized in our laboratories (unpublished results). 5-Fluorocytosine, 5-fluorouracil, cytosine, 1-pentanesulfonic acid sodium salt, and 1-heptanesulfonic acid sodium salt were purchased from Sigma Chemical Company (St. Louis, MO). Citric acid monohydrate was purchased from Fisher Scientific (Fair Lawn, NJ). HPLC grade acetonitrile, and granular ammonium sulfate were obtained from J.T. Baker (Phillipsburg, NJ). Triethylamine was obtained from Aldrich Chemical Company, Inc. (Milwaukee, WI).

Experimental Design. Five and six adult male Sprague-Dawley rats (Harlan Laboratories, Indianapolis, IN) weighing 309 ± 5.7 g, and 321 ±10.7 g (mean ± SD, p-value 0.05) were used for 5-FC, and A-5-FP studies respectively. Rats were housed in a 12 h light/12 h dark, constant temperature (22^{o}C) environment with free access to standard laboratory chow and water. Animals were acclimatized to this environment for 1 week before the experiment. On the day before the experiment, the external jugular veins of the rats were cannulated under ketamine: acepromazine : xylazine (50:3.3:3.3 mg/kg) anesthesia. The animals were fasted overnight, however, free access to water was allowed.

On the morning of the experiment, rats were placed in individual metabolism cages. 5-FC (50 mg/kg) or A-5-FP (60 mg/kg, an equimolar dose to 5-FC) was administered intravenously to each rat over a one-minute period via the cannula. About 0.3 ml blood samples were collected from the cannula into heparinized polypropylene microcentrifuge tubes prior to and at 0.08, 0.25, 0.5, 1, 1.5, 2, 3, 4, 6, 8, and 12 h after administration. Blood volume was replaced with an equal volume of normal saline. Blood samples were centrifuged at 9000g for 5 min and plasma was separated and frozen at -80^{o}C until analysis. Urine was collected for 24 h following the administration, its volume recorded, and frozen at -80^{o}C until analysis.

Analytical Methodology. An HPLC method was developed for the determination of the concentration of 5-FC, 5-FU, and A-5-FP simultaneously, in both plasma and urine. To 100 µL plasma in a polypropylene microcentrifuge tube were added 50 µL of internal standard solution (15 µg/ml cytosine), 50 µL water, and 800 µL ice-cold acetonitrile to precipitate plasma proteins. The mixture was vigorously mixed for about 30 s, and centrifuged for 3 min at 9000g. The supernatant was transferred to a clean tube and excess granular ammonium sulfate was added, mixed for 45 s, and centrifuged at 9000g for 5 min. Two layers separated, the lower of which was the aqueous layer. The top layer was transferred to a glass culture tube, and evaporated until dryness under a gentle stream of nitrogen gas at ambient temperature. The residue was reconstituted in 300 µL of mobile phase and 100 µL was injected onto the HPLC system.

For the determination of unchanged 5-FC, 5-FU and A-5-FP in urine, urine samples were diluted 1:100 with deionized water. A 100 µL of diluted urine were buffered with 50 µL of internal standard solution in 0.5 M phosphate buffer at pH 7.4 (15 µg/ml cytosine), and 50 µL water was added to the mixture. Buffering was necessary to keep the extraction conditions the same in all the samples. Urine sample preparation continued similar to plasma sample preparation.

Chromatography was performed on a Hypersil ODS column (5 m particle size, 4.6 X 250 mm; Alltech Associates Inc., Deerfield, IL) with a Nova-Pak C-18 online guard column (Waters Associates, Milford, MA).An isocratic mobile phase was used consisting of (3:97) acetonitrile:citric buffer solution containing 2.2 mM sodium pentanesulfonate, 1.8 mM sodium heptanesulfonate and 5 mM citric acid, and 17.5 µL triethylamine per liter of prepared mobile phase was then added. Flow rate was 1.5 ml/min, and the compounds were detected spectrophotometrically at a UV wavelength of 277 nm with detector range setting of 0.005 absorbance units, full scale, using a Waters Lambda-Max model 481 LC spectrophotometer (Waters Associates, Milford, MA). A Waters 712 WISP autosampler and a Waters Model 510 pump were used (Waters Associates, Milford, MA). The integrator used was D-2500 (LDC Analytical, Riviera Beach, FL).

The order of preparation and injection of the samples run in each day was randomized. The retention times of 5-FU, A-5-FP, 5-FC, and the internal standard were 2.9, 5.3, 6.2 and 11.2 min respectively. Baseline resolution was attained between all peaks of interest. Sample 5-FC, A-5-FP and 5-FU concentrations were calculated from the slope and intercept of calibration plots of the ratio between the peak area of each of the three compounds to the peak area of the internal standard versus standard concentration of each of the compounds. The slopes and intercepts were generated using weighted (1/conc) least-squares regression analysis.

Pharmacokinetic Analysis. Compartmental analysis was used to obtain pharmacokinetic parameters of 5-FC and A-5-FP. For both compounds, plasma concentrations were best described by a two-compartment open model. ADAPT-II was used to fit pharmacokinetic models to the data [11]. Parameter estimates for both compounds were generated from a fit to the two compartment linear model parameterized using clearances (2COMPCL) found in the ADAPT library of models, and Maximum Likelihood

estimation method was applied, where the slope of the variance model (σ_{slope}) was allowed to be estimated with an initial estimate of 0.1, and the intercept ($\sigma_{intercept}$) was fixed at zero μg/ml (Equations 2-4). The model was entered as a set of differential (Equations 2-1 and 2-2) and output (Equation 2-3) equations.

$$dx_1/dt = -(CLt/Vc + CLd/Vc) \bullet x_1(t) + (CLd/Vp) \bullet x_2(t) \quad (2\text{-}1)$$

$$dx_2/dt = (CLd/Vc) \bullet x_1(t) - (CLd/Vp) \bullet x_2(t) \quad (2\text{-}2)$$

$$y(t) = x_1(t)/Vc \quad (2\text{-}3)$$

$$\sigma^2 = (\sigma_{intercept} + \sigma_{slope} \bullet y(t))^2 \quad (2\text{-}4)$$

where x_1, x_2, *CLt*, *CLd*, *Vc* and *Vp* are the amount of the drug in the central compartment, the amount of the drug in the peripheral compartment, total clearance, distributional clearance, volume of the central compartment, and volume of the peripheral compartment, respectively. *y(t)* represents the concentration in the central compartment at time (*t*).

Initial estimates were generated by RSTRIP stripping procedure [12]. Steady-state volume of distribution (*Vss*) was calculated as (*Vc* + *Vp*). Renal clearance (*CLr*) was calculated as $f_e \times CLt$, where f_e is the fraction of the compound excreted unchanged in the urine. Nonrenal clearance (*CLnr*) was calculated as (*Clt* - *CLr*). Half-life, $t_{1/2}$, was calculated as (ln 2)/β, where β is defined as in Equation (2-5).

$$\beta = [(CLt/Vc+CLd/Vc+CLd/Vp)+\sqrt{(CLt/Vc+CLd/Vc+CLd/Vp)^2-4CLt\bullet CLd/Vc\bullet Vp)}]/2 \quad (2\text{-}5)$$

Statistical Analysis. For comparing parameter estimates of 5-FC and A-5-FP, nonparametric statistical procedure was applied. Two-tailed Wilcoxon Rank test with 95% confidence level was used.

Results and Discussion

The analytical methodology proved to be specific, linear, precise, and accurate over the range of concentrations encountered in this study. Calibration plots were linear in the range of 0.75 - 100, 0.25 - 100, and 0.5 - 75 μg/ml for 5-FC, A-5-FP and 5-FU, respectively, with R-square values not less than 0.97. The intraday relative standard deviations over the range of standard concentrations were <7%, and for the limit of quantitation <15%, for all 3 compounds. Mean intraday accuracy, calculated as mean calculated concentration/nominal concentration × 100, ranged between 86 - 103 %, and for the limit of quantitation between 80 - 120 %, for all 3 compounds. Interday relative standard deviations for low, medium, and high concentrations within the range of standard concentrations were less than 10%, for all 3 compounds. Mean interday accuracy ranged from 98 - 113% for all 3 compounds.

The mean plasma concentrations of 5-FC in 5 rats, and A-5-FP in 6 rats, in addition to a simulation based on the mean pharmacokinetic parameters for both compounds are shown in Figure 2-3. Pharmacokinetic parameters are listed in Table 2-1.

Unlike the case with azido-purine prodrugs, the azido-pyrimidine prodrug A-5-FP did not seem to convert to the amino counterpart, 5-FC as was expected. 5-FC was not detected in plasma after intravenous administration of A-5-FP to rats. Urinary excretion is the main route of elimination of 5-FC in rats [13], therefore, if a small amount of A-5-FP was converted to 5-FC, it might have been concentrated in the urine to a level exceeding the limit of quantitation. However, 5-FC was not detected in the urine. This might be due to the lack of specific reductive enzymes necessary to reduce the azide group to an amine function in azido-pyrimidine compounds. Direct conversion to 5-FU could be expected as an alternative pathway; however, 5-FU was not detected in plasma nor in urine. 5-FU is appreciably (21%) excreted in the urine [14].

Although A-5-FP showed similar volume of distribution at steady state, most other disposition parameters were significantly different from 5-FC. Volume of distribution at

steady state was close to 1 L/kg for both 5-FC and A-5-FP. This is greater than total body water (0.70 L/kg) in rats [15], which indicates intracellular distribution and perhaps entrapment by cellular binding. Total body clearance was higher for A-5-FP, while distributional clearance was lower. This was evident from the slower distributional phase and shorter terminal half-life seen in Figure 2-3. Both renal and nonrenal clearances were greater for A-5-FP. Renal clearance for both 5-FC and A-5-FP , 0.48 L/h/kg and 1.74 L/h/kg, respectively, were greater than glomerular filtration rate (0.27 L/h/kg) in rats [16], indicating active tubular secretion. In fact, the renal clearance of A-5-FP was similar to renal plasma flow rate (1.54 L/h/kg) in rats [16], indicating efficient active tubular secretion, with little or no tubular reabsorption, which is expected from the hydrophilic nature of the compound. Nonrenal clearance of 5-FC was low compared to A-5-FP at 0.13 L/h/kg and 0.87 L/h/kg, respectively. These results for 5-FC are consistent with previously published results [13], since 5-FC was not found to be metabolized to any appreciable degree in rats. It might be suggested, though, that A-5-FP is appreciably metabolized through a non-5-FC forming pathway.

Reference

1. Bennett JE. *Antifungal agents; in Goodman & Gillman (eighth ed): The Pharmacological Basis of Therapeutics.* New York, McGraw-Hill, 1990, 1168-1169.
2. Francis P, Walsh TJ. Evolving role of flucytosine in immunocompromized patients: New insights into safety, pharmacokinetics, and anti-fungal therapy. *Clin Infect Dis* 1992, **15**: 1003-1018.
3. Geige R, Weil JH. [tRNA's from yeast having incorporated 5-fluorouracil arising from in vivo deamination of 5-fluorocytosine]. Etude Des tRNA de levure ayant incorpore du 5-fluorouracile provenant de la desamination in vivo de la 5-fluorocytosine. *Bull Soc Chim Biol* 1970, **52**: 135-144.
4. Polak A, Scholer HJ. Mode of Action of 5-fluorocytosine and mechanisms of resistance. *Chemotherapy* 1975, **21**: 113-130.
5. Diasio RB, Bennett JE, Myers CE. Mode of action of 5-Fluorocytosine. *Biochemical Pharmacology* 1978, **27**: 703-707.
6. Bennet JE. Flucytosine. *Ann Intern Med* 1977, **86**: 319-322.
7. Dismukes WE, Cloud G, Gallis HA, Kerkering TM, Medoff G, Craven PC, Kaplowitz LG, Fisher JF, Gregg CR, Bowles CA, Shadomy S, Stamm AM, Diasio RB, Kaufman L, Soong SJ, Blackwelder WC, and the National Institute of Allergy and Infectious Diseases Mycoses Study Group. Treatment of cryptococcal meningitis with combination amphotericin B and flucytosine for four as compared with six weeks. *N Engl J Med* 1987, **317**: 334-341.
8. Stamm AM, Diasio RB, Dismukes WE, Shadomy S, Cloud GA, Bowles CA, Karam GH, Espinel-Ingroff A; Toxicity of amphotericin B plus flucytosine in 194 patients with cryptococcal meningitis. *Am J Med* 1987, **83**: 236-242.
9. Koudriakova T, Manouilov KK, Shanmuganathan K, Kotra LP, Boudinot FD, Cretton-Scott E, Sommadossi JP, Schinazi RF, Chu CK; *In vitro* and *in vivo*

evaluation of 6-azido-2',3'-dideoxy-2'-fluoro- -D-arabinofuranosylpurine and N^6-methyl-2',3'-dideoxy-2'-fluoro- -D-arabinofuranosyladenine as prodrugs of anti-HIV nucleosides 2'-F-ara-ddA and 2'-F-ara-ddI. *J Med Chem* 1996, **39**: 4676-4681.

10. Kotra LP, Manouilov KK, Cretton-Scott E, Sommadossi JP, Boudinot FD, Schinazi RF, Chu CK; Synthesis, biotransformation, and pharmacokinetic studies of 9-(-D-arabinofuranosyl)-6-azidopurine: A prodrug for ara-A designed to utilize the azide-reduction pathway. *J Med Chem* 1996, **39**: 5202-5207.
11. D'Argenio DZ, Schumitzky A. ADAPT II User's Guide: Pharmacokinetic/ Pharmacodynamic Systems Analysis Software. Biomedical Simulations Resource, Los Angeles, 1997.
12. RSTRIP II, MicroMath Inc., Salt Lake City, 1992.
13. Koechlin BA, Rubio F, Palmer S, Gabriel T, Duschinsky R. The metabolism of 5-fluorocytosine-2^{14}C and of cytosine-^{14}C in the rat and the disposition of 5-fluorocytosine-2^{14}C in man. *Biochemical Pharmacology* 1966, **15**: 435-446.
14. Jarugula VR, Lam SS, Boudinot FD. Nonlinear pharmacokinetics of 5-fluorouracil in rats. *J Pharm Sci* 1997, **86**: 756-758.
15. Gerlowski LE, Jain RK. Physiologically based pharmacokinetic modeling: Principles and applications. *J Pharm Sci* 1983, **72**: 1103-1127.
16. Patel BA, Chu CK, Boudinot FD. Pharmacokinetics and saturable renal tubular secretion of zidovudine in rats. *J Pharm Sci* 1989, **78**: 530-534.

Table 2-1. Mean (SD) pharmacokinetic parameters of 5-FC and A-5-FP after intravenous administration of equimolar doses of 50 and 60 mg/kg, respectively.

Parameter	**5-FC**	**A-5-FP**
No. of animals	5	6
CLt, L/h/kg	0.60 (0.07)	2.60 (0.21)[a]
CLr, L/h/kg	0.48 (0.11)	1.74 (0.25)[a]
CLnr, L/h/kg	0.13 (0.09)	0.87 (0.30)[a]
CLd, L/h/kg	1.85 (0.42)	0.49 (0.14)[a]
Vss, L/kg	0.99 (0.04)	1.11 (0.16)
Vc, L/kg	0.42 (0.11)	0.73 (0.09)[a]
Vp, L/kg	0.56 (0.08)	0.37 (0.13)
$t_{½}$, h	1.28 (0.16)	0.68 (0.17)[a]

[a] Significantly different from 5-FC value at 95% confidence level.

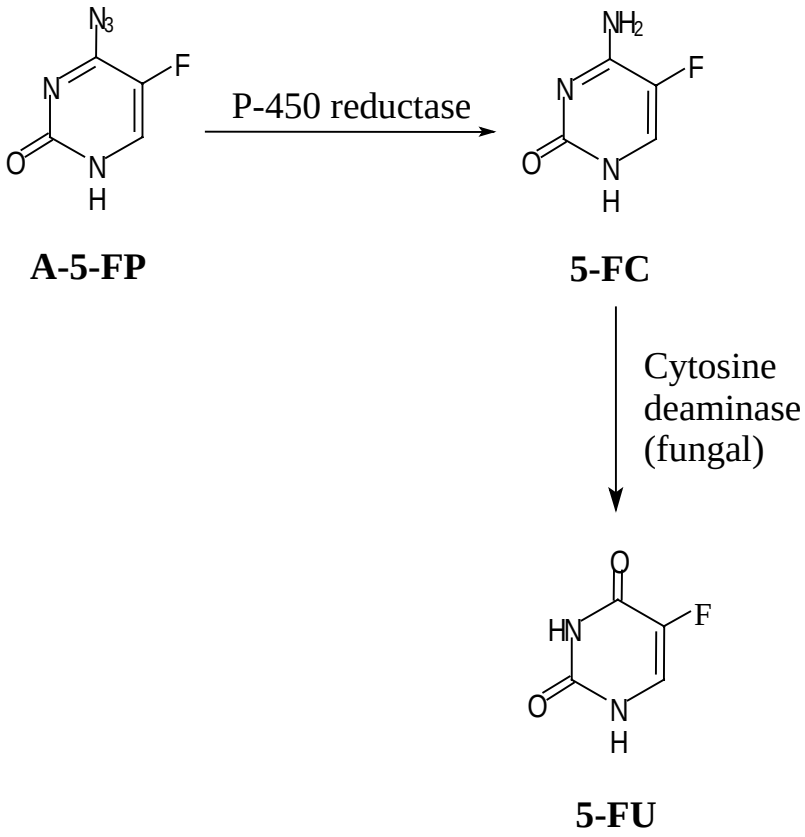

Figure 2-1. Hypothesizes biotransformation of A-5-FP.

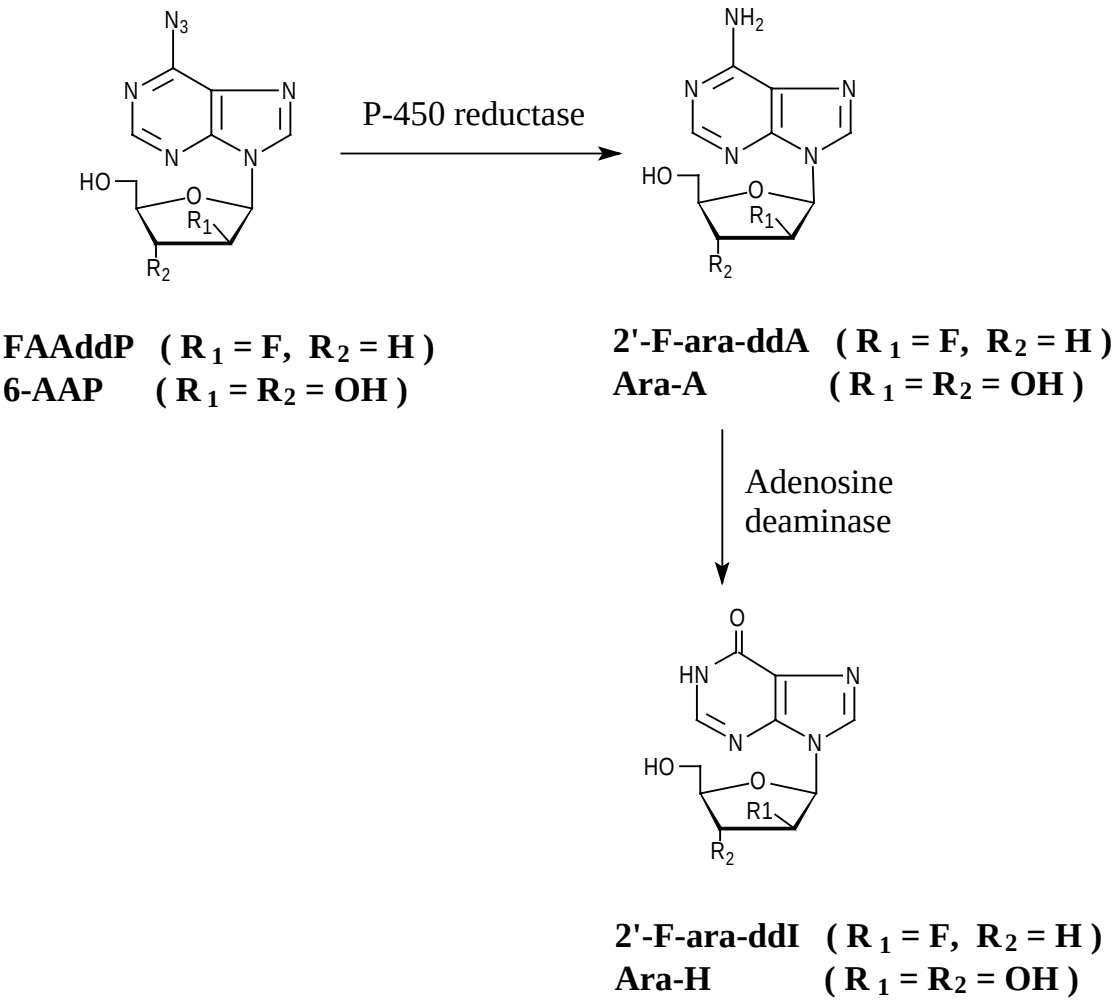

Figure 2-2. Biotransformation of prodrugs FAAddP and 6-AAP to 2'-F-ara-ddI and Ara-H, respectively.

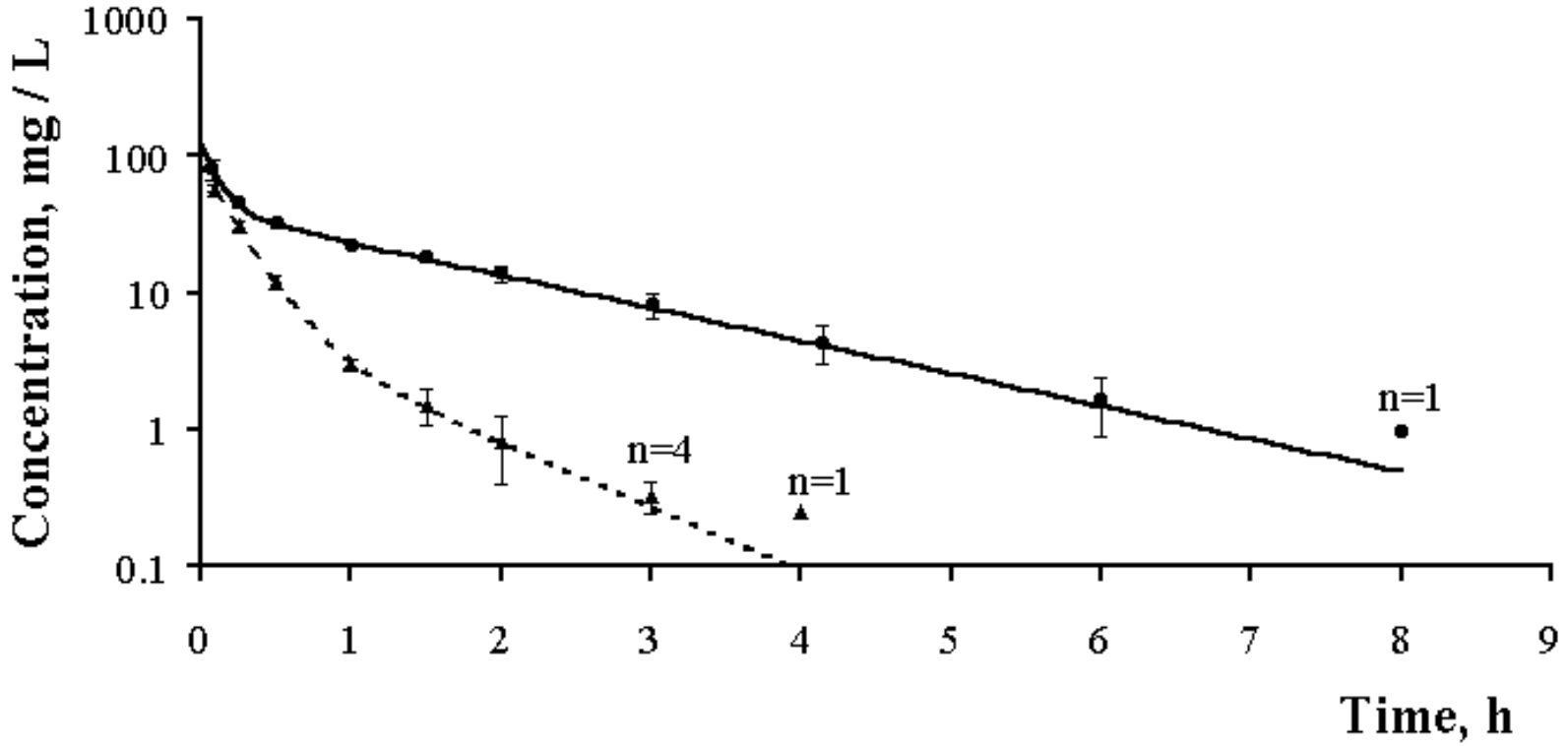

Figure 2-3. Mean (SD) plasma concentrations of 5-FC (●) and A-5-FP (▲) following intravenous administration of equimolar doses of 50- and 60-mg/kg, respectively, to rats. Symbols represent experimental data and lines represent simulated profiles based on average parameter values.

CHAPTER 3

STEREOSELECTIVE PHARMACOKINETICS OF 2´,3´-DIDEOXY-5-FLUORO-3´-THIACYTIDINE IN RATS[1]

[1]Eyas J. Abu-Raddad, David C. Delinsky, Michael G. Bartlett, Daniel B. Hall, Michael J. Otto, Raymond F. Schinazi, and F. Douglas Boudinot. Submitted to *Antimicrobial Agents and Chemotherapy*.

Abstract

The purpose of this investigation was to characterize the stereoselective pharmacokinetics of the R-(+)- and S-(−)-FTC enantiomers of the anti-HIV and anti-HBV agent 2´,3´-dideoxy-5-fluoro-3´-thiacytidine (RCV; Racivir™) in rats. A chiral electrophoretic (CE) method using 90 mM hydroxypropyl-*β*-cyclodextrin at pH 2.5 was used to determine enantiomer concentrations in plasma and urine. The analytical method was linear, selective, precise and accurate over the range of 0.5-100 μg/ml for both enantiomers. Three groups of 5 male rats (293 ± 13g, mean ± SD) were administered (+)-FTC, (−)-FTC or RCV intravenously and orally in a 2-period cross over study. Plasma and urine were collected and analyzed for individual enantiomer concentrations. Data for each enantiomer were modeled separately with a 2-compartment open model using nonlinear mixed effects modeling (NONMEM) to obtain pharmacokinetic parameter estimates. Data were then lumped and a model was constructed in a way to account and to test for pharmacokinetic differences between enantiomers and enantiomer-enantiomer interactions using the Wald test. Chiral inversion was not observed in vivo. Compared to (−)-FTC, (+)-FTC had 22% and 60% higher renal and nonrenal clearances, 90% and 31% higher central and steady-state volumes of distribution values, and 39% and 11% higher apparent absorption rate constant and bioavailability. A weak interaction between enantiomers was detected, reducing steady-state distribution volume by 29% and 9%, and slowing absorption by 32% and 27% for (+)- and (−)-FTC, respectively. In summary, the pharmacokinetics of RCV are characterized by slight to moderate stereoselectivity and weak enantiomeric interaction.

Keywords: FTC, RCV, dideoxycytidine, dideoxyfluorothiacytidine, stereoselective pharmacokinetics, chiral capillary electrophoresis, and hydroxypropyl-*β*-cyclodextrin.

Introduction

Additional pharmacotherapies for the treatment of hepatitis B virus (HBV) and human immunodeficiency virus (HIV) infections with improved pharmacological and toxicological profiles are needed.[32] Among the most potent compounds are 2′,3′-dideoxycytidine analogs, such as 2′,3′-dideoxy-3′-thiacytidine (BCH-189) and 2′,3′-dideoxy-5-fluoro-3′-thiacytidine, (RCV, Racivir™) that have shown high activity against HIV and HBV.[10,14,29-31,33] In general, the S-(−) enantiomers of BCH-189 and RCV, lamivudine (3TC; Epivir®) and emtricitabine ((−)-FTC; Coviracil®), corresponding to the unnatural L form, possess greater antiviral activity in cultured cells [9, 10,12,19, 23,29,31] than the corresponding R-(+) enantiomers.[12, 19, 29,31]

Owing to the chirality of biological environments, qualitative or quantitative differences in pharmacological action and disposition of enantiomers of chiral compounds often occur. Pharmacokinetic evaluations that do not use chiral assays may be misleading if the enantiomers have different dispositional properties, and may be blind to relevant issues such as chiral inversion and enantiomer-enantiomer interactions. Therefore, techniques to quantify individual enantiomers in pharmacokinetic samples should be implemented.[15] An increasing wealth of such techniques have been recently developed, utilizing high performance liquid chromatography (HPLC), gas chromatography (GC) and capillary electrophoresis (CE), among others.[3] The use of CE for chiral separation has attracted increasing interest due to very high efficiency, minimal peak broadening, the use of minute amount of analyte for sample injection, and the ease and speed with which the separation media can be changed during method development.[2] Modes of chiral separation in CE include host-guest complexation utilizing cyclodextrins (CDs) or crown ethers; electrokinetic chromatography utilizing optically active micelles; ligand exchange complexation utilizing metal complexes; complexation with oligosaccharides; and affinity electrokinetic chromatography utilizing proteins.[34]

RCV structure possesses two chiral centers, one of which is enantiomerically pure as the R configuration at 4′ position, and the other, at 1′ position, exists as R and S configurations, corresponding to the enantiomers R-(+)- and S-(−)-FTC, respectively (Figure 3-1). The pharmacokinetics of RCV and (−)-FTC have been investigated in mice,[18] rats,[1,17] cynomolgus monkeys,[18] woodchucks,[13] and rhesus monkeys.[28] Non-stereoselective assay of RCV and its enantiomers in plasma of mouse, rat and monkey and serum of woodchuck and monkey was performed using HPLC.[1,16-18, 28] Since stereoselective assay for the determination of (+)- and (−)-FTC in biological matrices has not yet been reported, the potential chiral inversion and enantiomeric interactions of FTC have not been addressed to date.

The purpose of this report is to describe the enantiomeric separation of R-(+)- and S-(−)-FTC for the determination of concentrations of each enantiomer in rat plasma and urine using hydroxypropyl-β-cycoldextrin-modified capillary electrophoresis and liquid-liquid extraction. This assay was employed to fully characterize and compare the pharmacokinetics of the enantiomers of RCV, namely (+)-FTC and (−)-FTC, including possible chiral inversion and enantiomer-enantiomer interactions, following intravenous and oral administration of RCV, (+)-FTC and (−)-FTC to rats.

Materials and Methods

Reagents and Chemicals. The individual enantiomers of RCV, as well as RCV, were supplied by Pharmasset. Enantiomeric purity was higher than 98 and 99% for (+)-FTC and (−)-FTC, respectively. Internal standard, 3TC, was obtained from the laboratory of Dr. Raymond F. Schinazi. Hydroxypropyl-β-cyclodextrin was obtained from Cerestar (Hammond, IN, USA). HPLC grade acetonitrile, phosphoric acid and granular ammonium sulfate were obtained from J.T.Baker Inc (Philipsburg, NJ, USA). Monobasic sodium phosphate was obtained from Merck (Germany). Blank rat plasma was obtained from Harlan Laboratories (Indianapolis, IN).

Analytical Methodology. Concentrations of (+)-FTC and (−)-FTC in plasma and urine were determined by an enantioselective capillary electrophoretic method. Stock solutions and serial dilutions of the compounds were prepared in deionized water to yield concentrations of 1000, 900, 250, 10 and 2.5 µg/ml of (+)- and (−)-FTC, and 60 µg/ml of S-(−)-2´,3´-dideoxy-3´-thiacytidine (3TC) as the internal standard. Appropriate volumes of stock solutions (10 or 20 µl) and 50 µl of internal standard solution were pipetted into a 1.5 ml microcentrifuge tube, along with an appropriate volume of rat plasma or 20-fold diluted urine to bring the total volume to 150 µl.

Sample preparation was performed using organic solvent protein precipitation followed by liquid-liquid extraction. To 150 µl plasma or diluted urine, internal standard and 600 µl ice-cold acetonitrile was added while mixing gently. The mixture was then vigorously mixed for 30 sec. Excess granular ammonium sulfate was added, and the mixture was mixed vigorously for 45 sec and centrifuged for 3 min at 9000 g. Two phases separated where the organic phase resided on top of an ammonium-sulfate-saturated aqueous layer. The organic phase was aspirated, transferred to a clean tube, evaporated to dryness under vacuum, and reconstituted in 75 µl of 30% (v/v) methanol in water.

Calibration curves were constructed using enantiomer concentrations of 0.5, 2.5, 10, 25, 75 and 100 µg/ml. Linear regression analysis of enantiomer to internal standard peak area ratio versus concentration, weighted by 1/concentration, gave slope and intercept estimates that were used to calculate the concentration of each enantiomer in plasma and diluted urine samples. The original concentration in urine was calculated by multiplying the resulting concentration by the dilution factor, 20. Precision and accuracy were determined at 0.5, 5 and 90 µg/ml in plasma for 3 days, and 0.5 and 90 µg/ml in urine in a single day.

Analysis was performed using a P/ACE System 5000 (Beckman Inc., Fullerton, CA) equipped with an UV detector. An uncoated fused silica capillary of total length of

37 cm, an effective length of 30 cm to the detector window, and 75 μm I.D. (Polymicro Technologies, Phoenix, AZ, USA) was used in the analysis. The capillary was thermostatted at 25 °C and the voltage was 25 kV. A 0.5 cm detection window was created by stripping the polyamide coating of the capillary. The detection was towards the cathodic end. The run buffer consisted of an aqueous solution of 90 mM hydroxypropyl-β-cyclodextrin in 50 mM phosphate buffer adjusted to pH 2.5 with concentrated phosphoric acid. The analytes were monitored at 280nm.

Sample introduction was performed using pressure injection for 5 sec at the high-pressure setting, followed by the application of high voltage ramping to 25 kV over 30 sec. Before each run, the capillary was rinsed under high pressure (5 PSI) for 2 min each with 0.1 M sodium hydroxide and run buffer solution.

Animals. Fifteen adult Sprague-Dawley rats weighing 293 ± 13 g (mean ± SD) were used for the study. Animals were housed in a 12-h light/12-h dark, constant temperature (22°C) environment with free access to standard laboratory chow and water in the University of Georgia College of Pharmacy Animal Care Facility, which is fully accredited by the American Association for the Accreditation of Laboratory Animal Care (AAALAC). Rats were acclimatized to this environment for at least one week before the study. Animal studies were approved by the University of Georgia Animal Care and Use Committee and conducted in accordance with guidelines established by the Animal Welfare Act and the National Institutes of Health Guide for the Care and Use of Laboratory Animals.

The right external jugular veins were cannulated under ketamine : acetopromazine : xylazine (50:3.3:3.3 mg/kg) anesthesia the day before the experiment. Rats were fasted overnight, with free access to water. On the day of the study, rats were individually placed in metabolism cages.

Pharmacokinetic study design and conduct. A crossover experimental design was implemented. The rats were randomized into three groups of 5 rats each. Each group received 33.7-56 mg of (+)-FTC, (−)-FTC, or RCV, both intravenously and orally, with one-week washout period. The order of administration was balanced within groups as much as possible. The animals were dosed with drug dissolved in 0.9% saline. Oral doses were administered with a feeding needle, and intravenous doses were administered via the cannula over 1-2 min, followed by rinsing with saline (0.5ml). It has been reported that RCV does not adsorb on the type of cannulae used in this study.[(1)]

Blood (0.4 ml) was drawn into heparinized microcentrifuge tubes before and at 0.083, 0.25, 0.5, 0.75, 1, 1.5, 2, 3, 4, 6 and 8 h after drug administration. Blood was replaced with an equal volume of normal saline. Blood samples were centrifuged at 2,000 x g for 5 min, and plasma was separated and frozen at –80°C until analysis. Urine samples were collected at 24 h after drug administration. Urine volume was recorded, and a portion of each sample was frozen at –80°C until analysis.

Data analysis. The three groups of animals, in addition to the ability to measure the enantiomers selectively in plasma and urine, produced four groups of data: (+)-FTC after (+)-FTC administration, (+)-FTC after RCV administration, (−)-FTC after (−)-FTC administration, and (−)-FTC after RCV administration. For each group, plasma concentrations and amount excreted in the urine were modeled with a two-compartment open model with first order absorption, for oral administration, and elimination. Physiologically parameterized, this model included the pharmacokinetic parameters of total body clearance (CL), volume of the central compartment (V_C), steady-state volume of distribution (V_{SS}), distributional clearance (CL_d), fraction excreted in the urine (F_u), apparent absorption rate constant (K_a), and oral bioavailability (F). Interindividual random effects were added to the pharmacokinetic parameters only when their addition

enhanced the fit. When added, the interindividual variability was modeled according to the logarithmic error model as (Equation 3-1).

$$\theta_{ni} = TV\theta_n \cdot exp[\eta_{ni}] \quad (3\text{-}1)$$

where θ_{ni} is the true value of the *n*-th pharmacokinetic parameter for the *i*-th individual (CL, Vc, Vss…etc.), $TV\theta_n$ is the typical value in the population, and η_{ni} is a subject-specific random variable with a mean of zero and variance of ω_n^2. Residual error variability for plasma measurements was modeled with a mixed proportional and additive error model (Equation 3-2).

$$C_{ij} = \hat{C}_{ij} (1 + \epsilon_{ij}) + \varepsilon_{ij} \quad (3\text{-}2)$$

where C_{ij} is the *j*-th measured plasma concentration in the *i*-th individual, $\hat{C}_j$ is the corresponding expected concentration, and ϵ_{ij} and ε_{ij} are independent, identically distributed statistical errors with zero means and covariance, and variances of δ^2 and σ^2, respectively. This model was used because high variability was observed at very low concentrations, which could not be explained by a proportional error model alone. Residual error variability for urine measurements was modeled with an additive error model. A separate run was also conducted with a reparameterized model to obtain renal and nonrenal clearances (CL_R and CL_{NR}, respectively). Fitting these and subsequent models was performed using the nonlinear mixed effects modeling program (NONMEM, version V level 1.1, University of California, San Francisco).[5] A representative NONMEM input file is included in Appendix A.

Hypothesis testing. Pharmacokinetic differences between the two enantiomers and the influence of the presence of one enantiomer (in racemic mixture) on the pharmacokinetics of the other were tested for significance using the Wald test.[35] The

following set of null hypotheses was constructed for each of the pharmacokinetic parameters of interest (CL, CL_R, CL_{NR}, V_C, V_{SS}, K_a and F):

H_1: There is no difference between the parameter value for (+)-FTC and that for (−)-FTC.

H_2: There is no influence on the parameter value of (+)-FTC due to the presence of (−)-FTC in the racemic mixture.

H_3: There is no influence on the parameter value of (−)-FTC due to the presence of (+)-FTC in the racemic mixture.

Plasma concentrations and the amount excreted in the urine for both (+)-FTC and (−)-FTC after administration of each enantiomer and RCV were lumped and modeled simultaneously with a physiologically parameterized two-compartment open model with first order absorption and elimination. Pharmacokinetic parameters were modeled as in Equation 3-3.

$$TV\theta_n = \mu_n + \beta_{1n} X_1 + \beta_{2n} X_2 + \beta_{3n} X_3 \qquad (3\text{-}3)$$

where μ_n is the overall parameter value in the population, and X_1, X_2 and X_3 are indicator variables where X_1 has a value 1 for (+)-FTC regardless of administered form and –1 otherwise, X_2 has a value of 1 for (+)-FTC after administration of (+)-FTC, –1 for (+)-FTC after RCV administration, and zero otherwise, and X_3 has a value of 1 for (–)-FTC after administration of (–)-FTC, –1 for (–)-FTC after administration of RCV, and zero otherwise. β_{1n}, β_{2n} and β_{3n} are parameters associated with the n-th pharmacokinetic parameter that have a value of zero under the null hypotheses H_1, H_2 and H_3, respectively. In this context, $\beta_{1n} = (\theta_{pp} + \theta_{pr}) - (\theta_{mm} + \theta_{mr})$, $\beta_{2n} = \theta_{pp} - \theta_{pr}$, and $\beta_{3n} = \theta_{mm} - \theta_{mr}$, where θ_{pp} is the specific parameter value for (+)-FTC after administration of (+)-FTC, θ_{pr} is the specific parameter value for (+)-FTC after RCV administration, θ_{mm} is the specific parameter value for (−)-FTC after administration of (−)-FTC, and θ_{mr} is the specific parameter value for (−)-FTC after administration of RCV.

Interindividual random effects were added to CL, K_a, and F according to the logarithmic error model described above. Residual error variability was modeled for plasma concentrations with a mixed proportional and additive error model, and for urine with an additive error model common to all 4 groups. NONMEM input file depicting this model is included in Appendix B.

Parameter estimates obtained by NONMEM are asymptotically normally distributed.[5] Therefore, the standard error (SE) of the estimate of β_{1n}, β_{2n} and β_{3n} obtained from NONMEM output, was used to test the two-tailed hypothesis that the estimate is equal to zero. A *P*-value less than 0.05 was considered significant, and subsequently, the null hypothesis was rejected.

Results

Baseline resolution of the enantiomers of FTC was achieved by CE using 90 mM hydroxypropyl-β-cyclodextrin. Retention times were 4, 12 and 13 min for 3TC, (+)-FTC and (−)-FTC, respectively. No interference from endogenous peaks was observed. The calibration curve in plasma and urine showed good linearity in the range of 0.5 to 100 µg/ml for both enantiomers. This range encompassed the typical range of concentrations encountered in the current study. The coefficients of determination obtained by linear regression were 0.999 or better. The intra-day precision and accuracy (n=6) in plasma samples, expressed as relative standard deviation (R.S.D. %) and % absolute bias were less than 3.4 and 5.7%, respectively, at concentrations above the lower limit of quantitation and less than 18.1 and 9.0%, respectively, at the lower limit of quantitation for both enantiomers. Inter-day precision and accuracy (n=18, over 3 days) were less than 3.1 and 4.7%, respectively, at concentrations above the lower limit of quantitation and less than 12.2 and 3.6%, respectively, at the lower limit of quantitation. Detailed precision and accuracy data for plasma samples are shown in Table 3-1. Precision and

accuracy for urine samples were less than 7.0 and 9.3%, respectively, for both enantiomers.

Plasma concentration profiles for (+)-FTC and (−)-FTC were comparable and differences between them were not readily visible. Figures 3-2 and 3-3 show the profiles for (+)-FTC and (−)-FTC following intravenous and oral administration, respectively, of each enantiomer and the racemic mixture. Model-predicted values are also depicted as lines. Low concentrations (<2%) of each of the enantiomers were detected at early time points after the administration of the other enantiomer, which could well be explained by the presence of each enantiomer as an impurity in the other enantiomer. Therefore, chiral inversion is highly unlikely.

The concentrations of both enantiomers exhibited biphasic declines following intravenous administration, where the first phase was relatively fast. In addition, visual inspection of overlayed intravenous and oral data (not shown) revealed that the terminal phase of decline after oral administration was significantly slower than that after intravenous administration for both enantiomers. Terminal phase half-lives of (+)-FTC and (−)-FTC calculated by nonlinear regression of the terminal phase was 1.5 and 2.1 h after oral administration and 0.6 and 0.8 h after intravenous administration, respectively. The effect of route of administration on half-life was found highly significant (*P*-value < 0.001; ANOVA), indicating flip-flop kinetics.

Pharmacokinetic parameter estimates for the four groups are displayed in Table 3-2. Interestingly, for one rat receiving (−)-FTC orally, absorption was profoundly faster than other rats in this group. Indeed, the K_a for this rat was approximately 4.5 fold higher than the mean K_a for the group, or more than 26 fold the standard deviation above the mean. When a model where K_a was modeled with proportional interindividual variability was fit to data for this group, variability jumped from 11% to 89% on the addition of this individual. However, estimates of all other pharmacokinetic parameters,

save K_a, were not significantly affected. Clearly this animal constituted an outlier, and subsequently, was eliminated from further parameter estimation or hypothesis testing.

Total, renal and nonrenal clearances, central compartment and steady-state volumes of distribution, apparent absorption rate constant and bioavailability were higher for (+)-FTC than for (−)-FTC with statistical significance. The magnitude of difference ranged from 11% for bioavailability to 90% for central compartment volume. The presence of the antipode in the racemic mixture slightly affected total clearance of (+)-FTC, a fact that was not manifested in either CL_R or CL_{NR}. Volumes of (+)-FTC seemed to be reduced by 29-43% in the presence of the antipode. The effect of (+)-FTC on the disposition of (−)-FTC was much less profound, if at all significant. On the other hand, absorption rate of both enantiomers was slowed in the presence of the antipode by 32 and 27% for (+)- (−)-FTC, respectively. The results of hypothesis testing are shown in Table 3-3.

Discussion

The structure of FTC offers an aromatic ring and multiple electrostatic interaction points close to the chiral center (Figure 3-1). Cyclodextrin-based chiral recognition is achieved by forming inclusion complexes where an aromatic or alkyl group is included into the CD cavity, and the hydroxyl groups at the rim of the CD cavity interact with substituent group on or near the chiral center of the analyte. Even though the electrophoretic mobilities of enantiomers are identical, when their binding constants to the cyclodextrin are different, they can be resolved.[2]

Baseline resolution of (+)- and (−)-FTC was achieved using 90 mM hydroxypropyl-β-cyclodextrin. Low pH was needed to ionize FTC. Although the pKa for FTC has not been reported, it has been reported for cytidine, cytosine and 5-fluorocytosine to be between 3.26 and 4.60.[24] Therefore, it is likely that FTC is appreciably ionized at a pH of 2.5, which allowed for its migration through the capillary

under conditions of high voltage. In addition, the selective ionization of FTC over its uridine counterpart, 2´,3´-dideoxy-5-fluoro-3´-thiauridine (FTU), a possible metabolite of FTC, allowed for separating interference due to FTU.

The lower detection limit was decreased by reconstituting the sample in low volume of a vehicle that has lower conductivity than the run buffer. Upon application of voltage during sample injection, a greater field will develop across the sample zone, causing the ions to migrate faster. When the ions reach the run buffer, the field decreases and they migrate more slowly. This occurs until the analytes are compressed into a smaller zone.[7,11] The lower limit of quantitation (LOQ) of 0.5 µg/ml was comparable to earlier HPLC methods developed for FTC that did not involve chiral separation.[16]

The organic protein precipitation and liquid-liquid extraction provided good sample clean-up, with no endogenous interferences. The CE method showed good linearity and precision within the range of 0.5-100 µg/ml. This method was suitable for the simultaneous determination of (+)-FTC and (−)-FTC in rat plasma and urine, and was employed to fully characterize and compare the pharmacokinetics of the R-(+) and S-(−) enantiomers of RCV.

Previous studies with pure enantiomers and RCV in mice, rats, woodchucks, and cynomolgus and rhesus monkeys have demonstrated enantiomeric and species differences in pharmacokinetics and metabolism. Renal excretion of the unchanged compound, accounting for 55-96% of the administered dose, was the predominant route of elimination for RCV in rats[1] and rhesus monkeys,[28] and for (−)-FTC in rats,[17] mice and cynomolgus monkeys.[18] Rapid deamination of (+)-FTC to 2,3'-dideoxy-5-fluoro-3'-thiauridine (FTU) was appreciable in rhesus monkeys,[28] and the main elimination pathway in woodchucks,[16] however, (−)-FTC was resistant to deamination. Tissue and blood of rhesus monkeys have a very high level of deaminase activity, whereas in humans this activity is found primarily in the liver. Rats, on the other hand, have no measurable deaminase activity.[8]

Although the stereoselective pharmacokinetics of RCV was studied in woodchucks,[16] chiral inversion and enantiomer-enantiomer interactions were not addressed due to the lack of enantioselective analytical method for biological samples. Chiral inversion has been reported for a few nonsteroidal anti-inflammatory agents in various species.[21] Nonetheless, previous reports suggested that chiral inversion of (−)-FTC did not occur in rhesus monkeys,[28] a fact that was confirmed in rats for both enantiomers of RCV in the current study.

The results of this pharmacokinetics study are in agreement with previous RCV and (−)-FTC studies in rats. Total and renal clearance were reported in rats at 1.9 and 1.1 L/h·kg for RCV,[1] and 1.8 and 1.5 L/h·kg for (−)-FTC,[17] compared to 2.1 and 1.2 L/h.kg for (+)-FTC, and 1.5 and 0.94 L/h·kg for (−)-FTC, on average, respectively, in the present study. The clearance of (+)-FTC was 37% higher than (−)-FTC, which was more due to higher nonrenal clearance (60%) than higher renal clearance (22%) of this enantiomer. In woodchucks, the clearance of (+)-FTC was more than tenfold higher than that of (−)-FTC. The discrepancy could well be explained by extensive deamination of (+)-FTC, which is highly improbable in rats due to the absence of deaminase activity,[8] and low renal clearance of both enantiomers characteristic of nucleoside renal elimination in woodchucks.[27,36] Renal clearance of both enantiomers was fourfold higher than the glomerular filtration rate in rats (0.27 L/h/kg),[26] indicating active secretory process, which has been previously observed for (−)-FTC in rats.[17] Due to the involvement of the optically active protein transporters, renal secretion could be expected to be affected by stereochemistry of RCV. However, the secretion of both enantiomers of RCV is highly efficient such that CL_R approaches renal plasma flow rate (1.5 L/h.kg),[20] and thus, only small difference between the enantiomers was observed (22%).

A small, but significant, difference between the enantiomers in the steady-state volume of distribution was observed. V_{SS} was 31% higher for (+)-FTC as compared to (−)-FTC. This is probably due to differences in the initial dilution volume (V_C), which

was 90% higher for (+)-FTC. Values for V_{SS} in the current study of 1.4 and 1.1 L/kg for (+)-FTC and (−)-FTC, respectively, are in accord with reported values at 2.2 and 1.5 L/kg for racemic and (−)-FTC, respectively. Further, V_{SS} was greater than that of total body water of the rat (0.7 L/kg)[20] indicating wide distribution of the compound.

In this study, absorption of (+)-FTC was faster (39% higher K_a), and slightly more complete (11% higher bioavailability) than that of (−)-FTC. In mice, the racemic mixture was absorbed faster than (−)-FTC.[6]

Enantiomer-enantiomer interaction has been reported for a number of compounds.[22,25] Competitive enantiomer-enantiomer protein binding, metabolism, transport, and enzyme induction or inhibition are some of the possible explanations for such an interaction. The absorption of both enantiomers was found to be faster after pure enantiomer administration compared to racemic mixture administration. The apparent absorption rate constant, K_a, was 46% and 37% higher after pure enantiomer versus racemic mixture administration for (+)-FTC and (−)-FTC, respectively. Many nucleoside analogs are transported by one or more of nucleoside transporters in the gastrointestinal tract.[4] Competitive transport could be the mechanism of interaction between the two enantiomers of RCV. It seems that this interaction did not affect the extent to which each of the enantiomers was absorbed. Enantiomer interaction effect on volumes was also detected for V_C of (+)-FTC and V_{SS} of both enantiomers. No interaction effect on renal or nonrenal clearances was detected.

In summary, RCV exhibits enantioselective absorption and disposition in rats. Renal and nonrenal clearance, steady-state and central compartment volumes of distribution, and rate and extent of absorption were all higher for the (+)-enantiomer. The magnitude of difference is not as profound as what was seen in woodchucks, mainly due to the absence of fast and extensive deamination of (+)-FTC in rats lacking deaminase activity. No chiral inversion was observed, and a weak interaction between the enantiomers was seen in absorption rate and volumes of distribution.

Acknowledgements

This work was supported in part by NIH grant AI-25899, Pharmasset, Inc., Tucker, GA and by the Department of Veterans Affairs (RFS).

References

1. Abobo, C. V., L. Ni, R. F. Schinazi, D. C. Liotta, and F. D. Boudinot. 1994. Pharmacokinetics of 2´,3´-dideoxy-5-fluoro-3´-thiacytidine in rats. J. Pharm. Sci. **83**:96-99.
2. Aboul-Enein H. Y., and I. W. Wainer (Editors), The Impact of Stereochemisty on Drug Development and Use, John Wiley & Sons. Inc., New York, NY, USA, 1997, p. 317.
3. Ariens E. J., in A. M. Krstulovic (Editor), Chiral Separation by HPLC, Applications to Pharmaceutical Compounds, Ellis Horwood Limited, W. Sussex, England, 1989, p. 31.
4. Balimane P. V., P. J. Sinko. 1999. Involvement of multiple transporters in the oral absorption of nucleoside analogs. Advanced Drug Delivery Reviews. **39**:183-209.
5. Beal S. L., L. B. Sheiner (eds.). NONMEM Users Guides. NONMEM Project Group, University of California, San Francisco.
6. Black, P.L., M. A. Ussery, M. J. Otto, L. Stuyver, S. J. Hurwitz, T. M. Barnett, J. O. Mowrey, P. M. Tharnish, F. D. Boudinot, and R. F. Schinazi. Antiviral activity of racivir™ and of emtricitabine in the HuPBMC-SCID mouse model of HIV infection, HIV DART 2000 (Frontiers in Drug Development for Antiretroviral Therapies), Abstract no. 17, San Juan, PR, December 2000.
7. Burgi D. S. and R. L. Chien. 1991. Optimization in sample stacking for high-performance capillary electrophoresis. Anal. Chem. **63**:2042-2047.

8. Camiener, G. W., and C. G. Smith. 1965. Studies of enzymatic deamination of cytosine arabinoside-I. Enzyme distribution and species specificity. Biochem. Pharmacol. **14:**1405-1416.

9. Cammack, N., P. Rouse, C. L. P. Marr, P. J. Reid, R. E. Boehme, A. V. Coates, C. R. Penn, and J. M. Cameron. 1992. Cellular metabolism of (−) enantiomeric 2′-deoxy-3′-thiacytidine. Biochem. Pharmacol. **43:**2059-2064.

10. Chang C.-N., S.-L. Doong, J. H. Zhou, J. W. Beach, L. S. Jeong, C. K. Chu, C. Tsai, and Y.-C. Cheng. 1992. Deoxycytidine deaminase-resistant stereoisomer is the active form of (±)-2′,3′-dideoxy-3′-thiacytidine in the inhibition of hepatitis B virus replication. J. Biol. Chem. **267:**13938-13942.

11. Chien R. L. and D. S. Burgi. 1991. Field amplified sample injection in high-performance capillary electrophoresis. J. Chromatogr. **559:**141-152.

12. Coates, J. A. V., N. Cammack, H. J. Jenkinson, I. M. Mutton, B. A. Pearson, R. Storer, J. M. Cameron, and C. R. Penn. 1992. The separated enantiomers of 2′-deoxy-3′-thiacytidine (BCH-189) both inhibit human immunodeficiency virus replication in vitro. Antimicrob. Agents Chemother. **36:**202-205.

13. Cullen, J. M., S. L. Smith, M. G. Davis, S. E. Dunn, C. Botteron, A. Cecchi, D. Linsey, D. Linzey, L. Frick, M. T. Paff, A. Goulding, and K. Biron. 1997. In vivo antiviral activity and pharmacokinetics of *cis*-5-fluoro-1-[2-(hydroxymethyl)-1,3-oxathiolan-5-yl]cytosine in woodchuck hepatitis virus-infected woodchucks. Antimicrob. Agents Chemother. **41:**2076-2082.

14. Doong S.-L., C.-H. Tsai, R. F. Schinazi, D. C. Liotta, and Y.-C. Cheng. 1991. Inhibition of the replication of hepatitis B virus *in vitro* by 2′,3′-dideoxy-3′-thiacytidine and related analogues. Proc. Natl. Acad. Sci. USA **88:**8495-8499.

15. FDA's policy statement for the development of new stereoisomeric drugs. 1992 Chirality **4**:338-340.

16. Fox, L. M., M. A. Ascenzi, B. C. Tennant, J. Shi, R. F. Schinazi, and F. D. Boudinot. Stereoselective pharmacokinetics and metabolism of 2´-deoxy-5-fluoro-3´-thiacytidine (FTC) in woodchucks. Submitted for publication.

17. Frick, L. W., L. St. John, L. C. Taylor, G. R. Painter, P. A. Furman, D. C. Liotta, E. S. Furfine, and D. J. Nelson. 1993. Pharmacokinetics, oral bioavailability, and metabolic disposition in rats of (−)-*cis*-5-fluoro-1-[2-(hydroxymethyl)-1,3-oxathiolan-5-yl]cytosine, a nucleoside analog active against human immunodeficiency virus and hepatitis B virus. Antimicrob. Agents Chemother. **37:**2285-2292.

18. Frick, L. W., C. U. Lambe, L. St. John, L. C. Taylor, and D. J. Nelson. 1994. Pharmacokinetics, oral bioavailability, and metabolism in mice and cynomolgus monkeys of (2´ *R*, 5´ *S*-)-*cis*-5-fluoro-1-[2-(hydroxymethyl)-1,3-oxathiolan-5-yl]cytosine, an agent active against human immunodeficiency virus and human hepatitis B virus. Antimicrob. Agents Chemother. **38**:2722-2729.

19. Furman P. A., M. Davis, D. C. Liotta, M. Paff, L. W. Frick, D. J. Nelson, R. E. Dornsife, J. A. Wurster, L. J. Wilson, J. A. Fyfe, J. V. Tuttle, W. H. Miller, L. Condreay, D. R. Averett, R. F. Schinazi, and G. R. Painter. 1992. The anti-hepatitis B virus activities, cytotoxicities, and anabolic profiles of the (−) and (+) enantiomers of *cis*-5-fluoro-1-[2-(hydroxymethyl)-1,3-oxathiolan-5-yl]cytosine. Antimicrob. Agents Chemother. **36:**2686-2692.

20. Gerlowski, L. E., and R. K. Jain. 1983. Physiologically based pharmacokinetic modeling: principles and applications. J. Pharm. Sci. **72:**1103-1127.

21. Jamali F, R Mehvar, F. M. Pasutto. 1989 Enantioselective aspects of drug action and disposition: therapeutic pitfalls. J. Pharm. Sci. **78:**695-715.

22. Lee E. J. D., K. Williams, R. Day, G. Graham, D. Champion. 1985. Stereoselective disposition of ibuprofen enantiomers in man. Br. J. Clin. Pharm. **19:**669-674.

23. Mathez, D., R. F. Schinazi, D. C. Liotta, and J. Leibowitch. 1993. Infectious amplification of wild-type human immunodeficiency virus from patients' lymphocytes and modulation by reverse transcriptase inhibitors in vitro. Antimicrob. Agents Chemother. **37:**2206-2211.

24. The Merck Index, 11th Edition, Merck and Co., Inc., Rahway, N.J., USA, 1989.

25. Murphy P. J, R. C. Nickander, G. M. Bellamy, and W. L. Kurtz. 1976. Effect of *l*-propoxyphene on plasma levels and analgesic activity of *d*-propoxyphene in the rat. J. Pharm. Exp. Ther. **199:**415-422.

26. Patel, B. A., C. K. Chu, F. D. Boudinot. 1989. Pharmacokinetics and saturable renal tubular secretion of zidovudine in rats. J. Pharm. Sci. **78:**530-534.

27. Rajagopalan, P., F. D. Boudinot, C. K. Chu, B. C. Tennant, B. H. Baldwin, and R. F. Schinazi. 1996. Pharmacokinetics of (−)-2′,3′-dideoxy-3′-thiacytidine in woodchucks. Antimicrob. Agents Chemother. **40**:642-645.

28. Schinazi, R. F., F. D. Boudinot, S. S. Ibrahim, C. Manning, H. M. McClure, and D. C. Liotta. 1992. Pharmacokinetics and metabolism of racemic 2′,3′-dideoxy-5-fluoro-3′-thiacytidine in rhesus monkeys. Antimicrob. Agents Chemother. **36**:2432-2438.

29. Schinazi R. F., C. K. Chu, A. Peck, A. McMillan, R. Mathis, D. Cannon, L. S. Jeong, J. W. Beach, W.-B. Choi, S. Yeola, and D. C. Liotta. 1992. Activities of the four optical isomers of 2′,3′-dideoxy-3′-thiacytidine (BCH-189) against human immunodeficiency virus type 1 in human lymphocytes. Antimicrob. Agents Chemother. **36:**672-676.

30. Schinazi R. F., D. C. Liotta, W.-B. Choi, A. Peck, H. McClure, F. D. Boudinot, J.-P. Sommadossi, M. Davis, P. A. Furman, and G. Painter. 1992. Cellular pharmacology and monkey pharmacokinetics of the antiviral (−)-2′,3′-dideoxy-5-fluoro-3′-thiacytidine (FTC). National Collaborative Drug Discovery Group, Frontiers in HIV Therapy, San Diego, Calif., Nov. 3-7, p. 59.

31. Schinazi R. F., A. McMillan, D. Cannon, R. Mathis, R. M. Lloyd, A. Peck, J.-P. Sommadossi, M. St. Clair, J. Wilson, P. A. Furman, G. Painter, W.-B. Choi, and D. C. Liotta. 1992. Selective inhibition of human immunodeficiency viruses by racemates and enantiomers of *cis*-5-fluoro-1-[2-(hydroxymethyl)-1,3-oxathiolan-5-yl]cytosine. Antimicrob. Agents Chemother. **36:**2423-2431.

32. Schinazi R. F., J. R. Mead, P. M. Feorino. 1992. Insights into HIV chemotherapy. AIDS Res. Hum. Retroviruses **8:**963-990.

33. Soudeyns H., X.-J. Yao, Q. Gao, B. Belleau, J.L. Kraus, N. Nguyen-ba, B. Spira, and M. A. Wainberg. 1991. Anti-human immunodeficiency virus type 1 activity and in vitro toxicity of 2´-deoxy-3´-thiacytidine (BCH-189), a novel heterocyclic nucleoside analog. Antimicrob. Agents Chemother. **35:**1386-1390.

34. Terabe S., K. Otsuka and H. Nishi, 1994. Separation of enantiomers by capillary electrophoretic techniques. J. Chromatogr. A, **666**:295-319.

35. Wald A. 1943. Tests of statistical hypotheses concerning several parameters when the number of observations is large. Trans. Am. Math. Soc. **54**:426-482.

36. Witcher, J. W., F. D. Boudinot, B. H. Baldwin, M. A. Ascenzi, B. C. Tennant, J. F. Du, and C. K. Chu. 1997. Pharmacokinetics of 1-(2-fluoro-5-methyl-β-L-arabinofuranosyl)-uracil (L-FMAU) in woodchucks. Antimicrob. Agents Chemother. **41**:2184-2187.

Table 3-1. Precision and accuracy of the CE method for the determination of (+)-FTC and (−)-FTC in plasma samples.

Concentration			***R.S.D. (%)***		***Absolute bias (%)***	
(μg/ml)	***Day***	***n***	***(+)-FTC***	***(−)-FTC***	***(+)-FTC***	***(−)-FTC***
Intra-day						
0.5	1	5	6.7	2.9	6.8	2.5
	2	6	13.0	11.1	2.1	8.9
	3	6	10.4	18.1	1.9	2.1
5	1	6	3.0	3.4	5.5	5.7
	2	6	2.4	2.8	5.5	5.3
	3	6	2.2	1.9	3.0	2.0
90	1	6	1.2	1.4	2.7	3.4
	2	6	0.6	0.6	1.1	1.5
	3	6	2.3	2.7	1.4	2.0
Inter-day						
0.5		18	10.5	12.1	2.1	3.5
5		18	2.7	3.1	4.7	4.3
90		18	1.6	1.8	1.7	2.3

Table 3-2. Pharmacokinetic parameter estimates (95% confidence interval) for (+)-FTC and (−)-FTC following intravenous and oral administration of (+)-FTC, (−)-FTC, and RCV.

Parameter	***(+)-FTC after (+)-FTC***	***(+)-FTC after RCV***	***(−)-FTC after (−)-FTC***	***(−)-FTC after RCV***
CL, L/h	0.64 (0.60-0.68)	0.60 (0.56-0.63)	0.45 (0.44-0.47)	0.44 (0.42-0.46)
CL_R, L/h	0.34 (0.31-0.37)	0.34 (0.22-0.45)	0.30 (0.29-0.32)	0.25 (0.16-0.34)
CL_{NR}, L/h	0.30 (0.26-0.33)	0.25 (0.15-0.34)	0.15 (0.12-0.18)	0.19 (0.11-0.27)
V_C, L	0.37 (0.28-0.39)	0.21 (0.15-0.28)	0.15 (0.13-0.17)	0.16 (0.14-0.18)
V_{SS}, L	0.49 (0.39-0.58)	0.35 (0.29-0.41)	0.33 (0.31-0.36)	0.30 (0.27-0.34)
K_a, h^{-1}	0.70 (0.62-0.78)	0.48 (0.39-0.57)	0.49 (0.42-0.56)	0.36 (0.28-0.43)
F	0.79 (0.68-0.90)	0.83 (0.71-0.95)	0.69 (0.66-0.72)	0.77 (0.70-0.83)

Table 3-3. Evaluation of pharmacokinetic differences between the enantiomers of RCV and the influence the presence of the antipode in the racemic mixture on the pharmacokinetics of both enantiomers.

Parameter	*Hypothesis:* **Underlying question**	**Estimate**†	**C.V.** ‡	***P*-value**§	**Conclusion**	**Magnitude**¥
CL	H_1:Enantiomer difference in CL?	0.084	8.3	<0.0001	Yes	1.37
	H_2:Influence of (−)-FTC on CL of (+)-FTC?	0.036	47.5	0.035	Yes	0.92
	H_3:Influence of (+)-FTC on CL of (−)-FTC?	0.0083	102.4	0.329	No	
CL_R	H_1:Enantiomer difference in CL_R?	0.024	18.0	<0.0001	Yes	1.22
	H_2:Influence of (−)-FTC on CL_R of (+)-FTC?	-0.001	2372.1	0.966	No	
	H_3:Influence of (+)-FTC on CL_R of (−)-FTC?	0.034	73.3	0.173	No	
CL_{NR}	H_1:Enantiomer difference in CL_{NR}?	0.060	12.4	<0.0001	Yes	1.60
	H_2:Influence of (−)-FTC on CL_{NR} of (+)-FTC?	0.037	71.7	0.163	No	
	H_3:Influence of (+)-FTC on CL_{NR} of (−)-FTC?	-0.026	84.3	0.236	No	
V_C	H_1:Enantiomer difference in V_C?	0.034	31.8	0.0017	Yes	1.90
	H_2:Influence of (−)-FTC on V_C of (+)-FTC?	0.050	24.8	0.0001	Yes	0.57
	H_3:Influence of (+)-FTC on V_C of (−)-FTC?	0.009	54.2	0.065	No	

† The estimate of β_{1n}, β_{2n} and β_{3n}.

‡ The coefficient of variation of the estimate (%) = 100 · (SE of estimate/parameter estimate).

§ *P*-value for the two-tailed test of the hypothesis that the estimate is equal to zero.

¥ Ratio of (+)-FTC to (−)-FTC, or racemate administration to pure enantiomer administration, as suitable.

Table 3-3 (cont'd). Evaluation of pharmacokinetic differences between the enantiomers of RCV and the influence the presence of the antipode in the racemic mixture on the pharmacokinetics of both enantiomers.

Parameter	*Hypothesis:* **Underlying question**	**Estimate**†	**C.V.** ‡	***P*-value**§	**Conclusion**	**Magnitude**¥
V_{SS}	H_1*:*Enantiomer difference in V_{SS}?	0.027	14.0	<0.0001	Yes	1.31
	H_2*:*Influence of (−)-FTC on V_{SS} of (+)-FTC?	0.054	19.1	<0.0001	Yes	0.71
	H_3*:*Influence of (+)-FTC on V_{SS} of (−)-FTC?	0.020	50.1	0.046	Yes	0.91
K_a	H_1*:*Enantiomer difference in K_a?	0.060	25.3	0.0001	Yes	1.39
	H_2*:*Influence of (−)-FTC on K_a of (+)-FTC?	0.090	36.8	0.0065	Yes	0.68
	H_3*:*Influence of (+)-FTC on K_a of (−)-FTC?	0.073	47.6	0.0356	Yes	0.73
F	H_1*:*Enantiomer difference in F?	0.064	32.0	0.0018	Yes	1.11
	H_2*:*Influence of (−)-FTC on F of (+)-FTC?	0.007	656.9	0.879	No	
	H_3*:*Influence of (+)-FTC on F of (−)-FTC?	-0.037	61.1	0.1017	No	

† The estimate of β_{1n}, β_{2n} and β_{3n}.

‡ The coefficient of variation of the estimate (%) = 100 · (SE of estimate/parameter estimate).

§ *P*-value for the two-tailed test of the hypothesis that the estimate is equal to zero.

¥ Ratio of (+)-FTC to (−)-FTC, or racemate administration to pure enantiomer administration, as suitable.

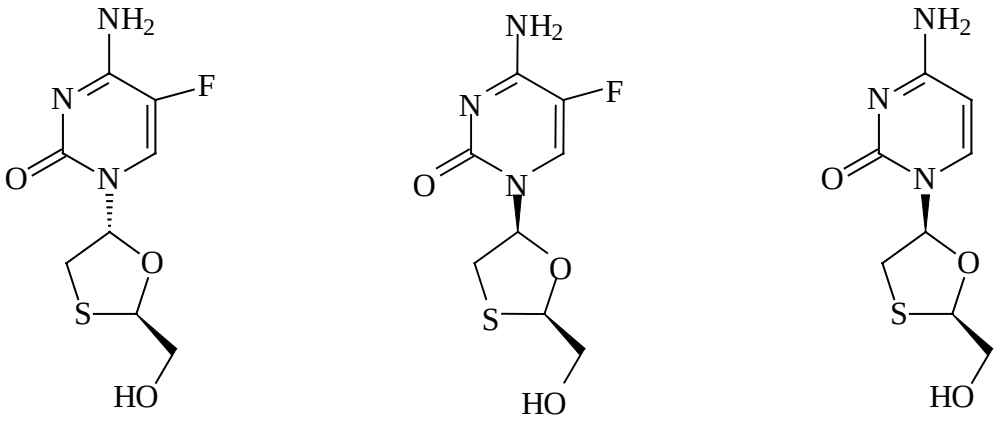

Figure 3-1. Chemical structures of enantiomers of RCV, and 3TC (internal standard).

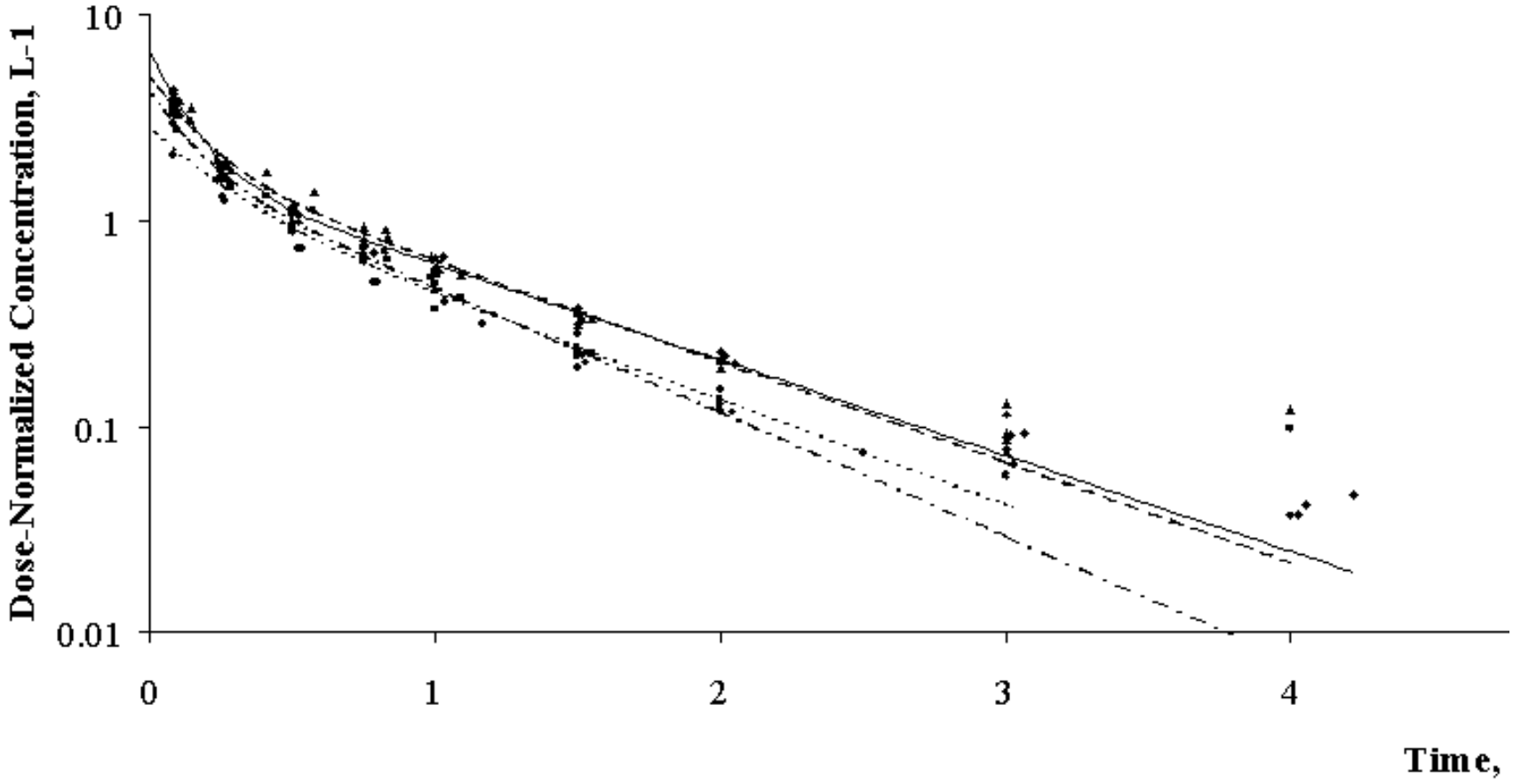

Figure 3-2. Dose normalized plasma concentrations (symbols) and model predictions (lines) of (−)-FTC (◆—◆) following intravenous administration of (−)-FTC, (−)-FTC (▲---▲) following intravenous administration of RCV, (+)-FTC (●·····●) following intravenous administration of (+)-FTC, and (+)-FTC (■-·-·-■) following intravenous administration of RCV.

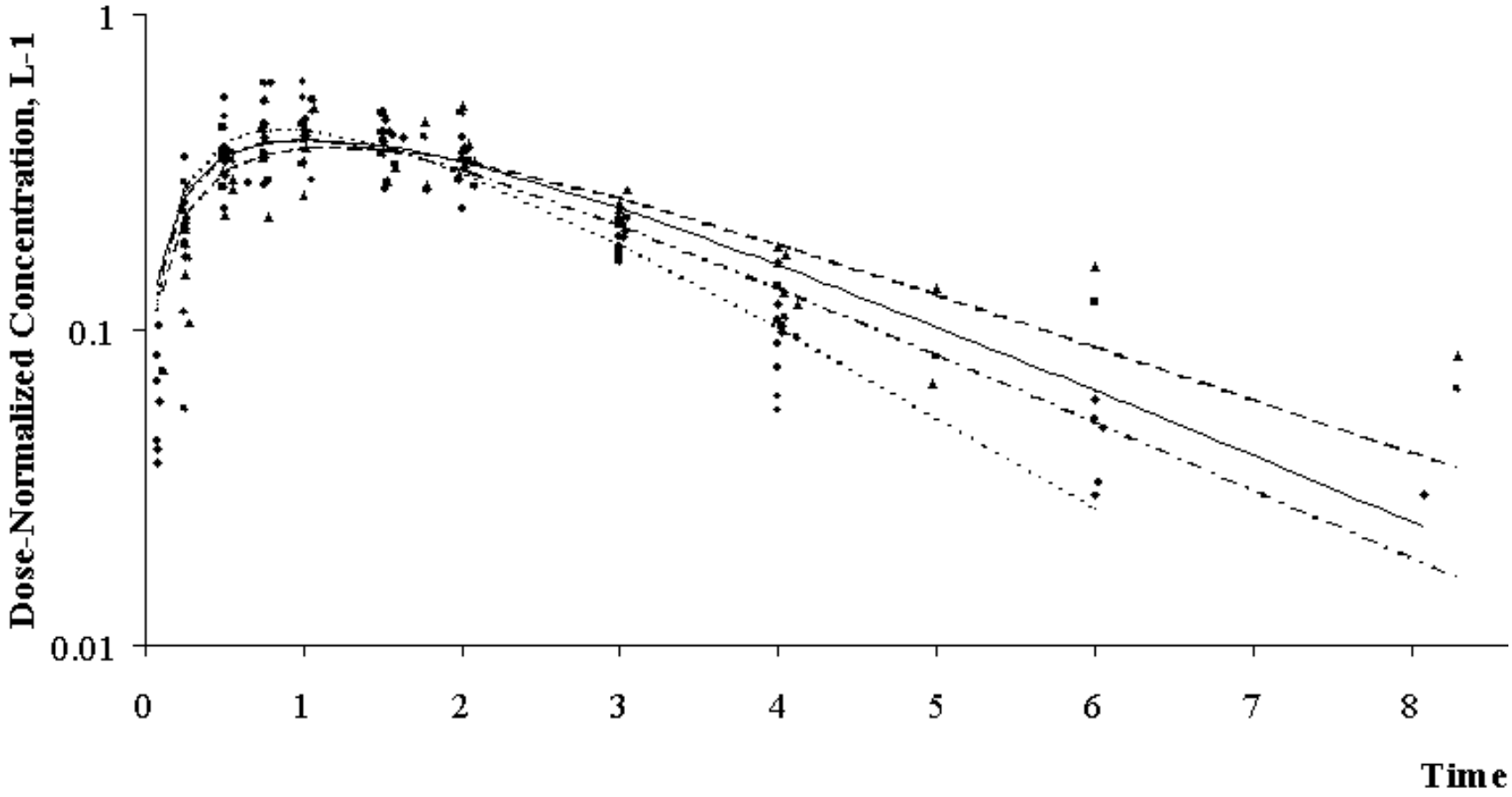

Figure 3-3. Dose normalized plasma concentrations (symbols) and model predictions (lines) of (−)-FTC (◆—◆) following oral administration of (−)-FTC, (−)-FTC (▲---▲) following oral administration of RCV, (+)-FTC (●·····●) following oral administration of (+)-FTC, and (+)-FTC (■-·-·-■) following oral administration of RCV.

CHAPTER 4

THE APPLICATION OF NONLINEAR MIXED EFFECTS MODELING (NONMEM) IN ALLOMETRIC INTERSPECIES SCALING OF S-(−)-2′,3′-DIDEOXY-5-FLUORO-3′-THIACYTIDINE[1]

[1]Eyas J. Abu-Raddad and F. Douglas Boudinot. To be submitted to *Pharmaceutical Research*.

Abstract

Allometry has been successfully used to predict clinical PK properties of nucleoside analogues, due to highly efficient renal excretion, and low plasma protein binding. The purpose of this report is to characterize the allometric relationships that explain species differences in the pharmacokinetics (PK) of S-(−)-2',3'-dideoxy-5-fluoro-3'-thiacytidine ((−)-FTC; emtricitabine), a nucleoside analogue with high activity against human immunodeficiency and hepatitis B viruses (HIV and HBV, respectively). PK time profiles were obtained for (−)-FTC in mice, rats, woodchucks and rhesus monkeys from the literature. Nonlinear mixed effects modeling (NONMEM) was used to estimate PK properties of a 2-compartment open model in each species separately, namely total (CL), renal (CLr), nonrenal (CLnr) and distributional (CLd) clearances, and central (Vc) and peripheral (Vp) volumes. Data were then lumped and body weight was introduced to the PK parameter models as a covariate according to the allometric relationship, $Y_i=aW_i^b$, where Y_i is the PK property (clearances and volumes), W_i is body weight, and a and b are the allometric coefficient and exponent. The initial fit was deficient, and mispredicted all species. Based on low renal clearance of nucleoside analogues reported in the literature, clearance for woodchuck was singled out of the allometric relationship. The fit was improved significantly for all species, especially for woodchuck, however, a systematic underprediction of woodchuck data, and overprediction of its PK parameters persisted. As hibernating animals, woodchucks are known to contain a higher and circannually changing adipose tissue fraction of body weight. Subsequently, a parameter was introduced to the model as a multiplier of woodchuck body weight, and was estimated. The fit was enhanced tremendously for all species. Data and PK parameters were predicted with a higher accuracy, and the allometric exponents were 0.784, 0.993, 1.00, 0.713 for CL, Vc, Vp and CLd, respectively, closely in agreement and not significantly different than the theoretical values of ¾ for functional properties like clearances, and 1 for structural properties like volumes (West et al 1997, Peters 1983). The mixed effects

model predicted PK properties for a 70-kg man to be 27.7 and 21.5 L/h for CL and CLd, and 40.3 and 32.8 L for Vc and Vp, respectively. The accuracy of this prediction remains to be verified. In conclusion, the use of the knowledge base for a new chemical entity and the animal models it is tested in can better explain pharmacokinetic interspecies differences, which in turn may help predict human pharmacokinetics more accurately.

Keywords: FTC, RCV, Dideoxyfluorothiacytidine, Pharmacokinetics, Allometric interspecies scaling, NONMEM.

Introduction

2′,3′-Dideoxycytidine analogs, such as 2′,3′-dideoxy-5-fluoro-3′-thiacytidine (RCV, Racivir™), have shown high activity against human immunodeficiency virus (HIV) and hepatitis B virus (HBV).[1-6] The S-(−) enantiomers of RCV, emtricitabine ((−)-FTC; Coviracil®), corresponding to the unnatural L form, possess greater antiviral activity [2,4,5,7-10] and lower toxicity to bone marrow stem cells and other cultured cells than the (+) enantiomers.[2,5,7,9] (−)-FTC is in the clinical stages of development, and has shown encouraging efficacy against HIV and HBV infections, and good tolerability.[11-13]

Pharmacokinetics of (−)-FTC has been investigated in mice,[14] rats,[15,16] rhesus[17] and cynomolgus monkeys,[14] and woodchucks.[18] In general, the compound showed biphasic disposition after intravenous administration, distributed widely into total body water, and was mainly cleared renally except in woodchucks.

Interspecies scaling of pharmacokinetic properties obtained from preclinical studies, has often been successful in predicting drug disposition in man, leading to significant time savings in clinical drug development.[19] Although other approaches for scaling exist, the allometric approach has been the most commonly used; due to simplicity and practicality, because only little information is required, that are usually acquired during regular preclinical development of new chemical entities.

Allometry, relating physiological and anatomical propertied to body size stem from the fact that humans share many similarities in anatomy, physiology, and biochemistry with other mammals, and the most obvious difference is size and shape.[20] Many anatomical and physiological properties (*Y*) can be described as a function of body weight (*W*; a surrogate of size), using the power model, $Y = a\ W^b$, where *a* and *b* are the coefficient (the value of Y when W is 1) and the exponent of the allometric relationship, respectively.[21] Due to the dependence on physiological processes and anatomical spaces, the clearance and distribution of xenobiotics can often be related to size in a similar fashion. Commonly encountered values for the exponents are ¾ for functions (like

clearances and metabolic rates), and 1 for volumes.[21] Theories behind these values have been suggested, the latest of which was based on how essential materials are transported through space-filling fractal networks of branching tubes, and assumes that the energy dissipated is minimized, and that the terminal tubes do not vary with body size.[22]

Establishing allometric relationship has traditionally been conducted by obtaining pharmacokinetic parameters for multiple species using noncompartmental analysis methods, followed by linear regression of log-transformed parameters on log-transformed body weight. Dedrick et al[23] have superimposed plasma concentrations from different species by converting chronological time to “time equivalents”, subsequently termed “pharmacokinetic time”,[24] based on the premise that different species dispose of drug molecules at rates correlated with internal physiological processes. Nonlinear regression analysis on Dedrick’s plots produces a species-invariant pharmacokinetic characterization, from which the dispositional properties can be rescaled to each species by back converting to chronological time. Most recently, nonlinear mixed effects modeling (NONMEM) has been used to characterize allometric dependence of pharmacokinetic properties.[25-29] The ability to obtain allometric coefficients and exponents in a single step, and the flexibility of adding more complicated covariate and statistical structures, make NONMEM a more plausible approach.

In this report, we describe an endeavor to establish an allometric relationship that explains differences between 4 species in the pharmacokinetics of (−)-FTC. Species-specific information are accounted for and incorporated in such a relationship, and the premise that pharmacokinetic properties scale allometrically to exponents of ¾ and 1 for functions and volumes, respectively, is tested.

Methods

Data from studies in adult male mice,[14] rats,[16] rhesus monkeys, [17] and woodchucks[18] were used. Individual serum or plasma and cumulative urine observations were obtained for rats, monkeys and woodchucks, and average plasma and cumulative urine observations were obtained for mice. Only data after intravenous administration were used. Linearity has been established for the doses used in these reports. A descriptive summary of the data used is shown in Table 4-1.

Pharmacokinetic parameters for each species were obtained using the nonlinear mixed effects modeling software package running on a PC station with Windows NT operating system (NONMEM, version V level 1.1; University of California, San Francisco, California).[30] For each species, a 2-compartment open model with first order elimination was fit to the data. Physiologically parameterized, it included the pharmacokinetic parameters of clearance (CL), distributional clearance (CLd), central compartment volume (Vc) and peripheral compartment volume (Vp) (ADVAN3 TRANS4). With urine data added, the model was reparameterized for renal and nonrenal clearances (CLr and CLnr, respectively), where CLr equals the total clearance multiplied by the fraction excreted in the urine (Fu), and CLnr equals the difference between CL and CLr. Then data from all animals were pooled and modeled simultaneously, where body weight (W) was a covariate for all pharmacokinetic parameters according to the allometric equation (Equation 4-1).

$$TVP_{ni} = a_n W_i^{bn} \qquad (4\text{-}1)$$

where TVP_{ni} is the value of the n-th pharmacokinetic parameter for a typical individual of body weight (W_i), a_n is the allometric coefficients (the typical value for an individual of a unit body weight), b_n is the allometric exponent of body weight (W). Interindividual variability was modeled using the logarithmic error model (Equation 4-2).

$$P_{ni} = TVP_{ni} \cdot exp[\eta_{ni}] \quad (4\text{-}2)$$

where P_{ni} is the value of the n-th pharmacokinetic parameter for the i-th individual, and η_{ni} is a subject-specific random variable with a mean of zero and a variance covariance matrix of ω_n^2. Residual variability in plasma/serum concentrations was modeled by a mixed proportional and additive error model (Equation 4-3).

$$C_{ij} = \hat{C}_{ij} (1 + \epsilon_{ij}) + \varepsilon_{ij} \quad (4\text{-}3)$$

where C_{ij} is the j-th measured plasma concentration in the i-th individual, $\hat{C}_{ij}$ is the corresponding expected concentration, and ϵ_{ij} and ε_{ij} are independent, identically distributed random variables with zero means and covariance, and variances of δ^2 and σ^2, respectively. When added, urine observations were modeled with an additive residual error model.

A number of models were fit to the data to address specific questions, and test various hypotheses. A representative NONMEM input file describing one of these models is included in Appendix C. The objective function was minimized using the FOCE (first order conditional estimation) method with interaction. Hypothesis testing was conducted using the likelihood ratio test (LRT).[31] The minimum value of the objective function determined in NONMEM fitting routine is equal to −2 log likelihood. The difference in −2 log likelihood values between nested models (LLD) is asymptotically distributed as chi-square with degrees of freedom equal to the difference in the number of freely estimated parameters between the two models.[30] A log likelihood difference associated with a P value of <0.05 was deemed significant, and subsequently, the corresponding null hypothesis was rejected.

Results

The decline of (−)-FTC concentration in plasma and serum after intravenous administration was biphasic in all species. Observed and model-predicted pharmacokinetic profiles of (−)-FTC in mice, rats, woodchucks and rhesus monkeys are shown in Figure 4-1. Pharmacokinetic parameter estimates for the 2-compartment open model obtained from each species separately are included in Table 4-1. The estimates are in general agreement with published estimates for (−)-FTC in mice, rats, woodchucks and rhesus monkeys.[14-18] A general increasing trend of all parameters with body weight is obvious.

Figure 4-2 shows the "elementary" Dedrick's plot of dose-normalized concentrations of (−)-FTC *vs.* pharmacokinetic time (chronological time divided by body weight raised to the power 0.25). Data from mice, rats and monkeys were superimposable, but woodchuck data were underpredicted by the Dedrick's plot of other species.

A 2-compartment model with body weight as a covariate of all pharmacokinetic parameters according to the allometric model was fit to the pooled data (**model I**). The residual proportional error was low (8.8%), accounting for measurement error, intraindividual variability and model misspecification. Interindividual variability was relatively high for CL and Vc at 37 and 25%, respectively, and low for Vc and CLd at 15 and 3.5%, respectively. The model systematically overpredicted monkey and rat observations, and underpredicted woodchuck and mouse observations. Woodchuck observations were the most poorly predicted. Observed *vs.* predicted plots for this model are shown in Figure 4-3. The estimates of allometric exponents were 0.69, 0.93, 0.94 and 0.65 for CL, Vc, Vp, and CLd, respectively. Fixing the exponents to the theoretical values enhanced the predictions for mouse, rat and monkey, while predictions for woodchuck worsened. The minimum value of the objective function (OFV) increased by 10.399 units, which allows us to reject the hypothesis that all the exponents are equal to

their theoretical value (*P*-value 0.034; LRT with 4 degrees of freedom). Fixing the exponent of each parameter at a time increased the OFV by values associated with *P*-values of 0.04, 0.12, 0.09, and 0.04 for CL, Vc, Vp and CLd, respectively. CL, Vc, Vp and CLd were all overestimated for woodchuck, but the estimate of CL suffered the most. These results are consistent with the fact that woodchuck was an outlier in the elementary Dedrick's plot (Figure 4-2). Removing woodchuck data (**model II**) enhanced the fit appreciably, with residual variability of 8.4%, interindividual variability less than 21% for all pharmacokinetic parameters, and better prediction of observations. Collectively, these findings were in favor of considering woodchuck an allometric outlier, at least for the clearance of (−)-FTC.

To explore the hypothesis that (−)-FTC clearance in woodchuck is an allometric outlier, while other pharmacokinetic parameters are not, **model III** was fit to the data, in which a unique CL value for woodchuck was singled out of the allometric relationship for CL, and was allowed to be estimated along with the allometric parameters. Other parameters were scaled according to the allometric relationship including all four species. The OFV dropped 18.414 points (*P*-value < 0.0001; LRT with 1 degrees of freedom), interindividual variability in CL dropped to 27%, and the estimates of the allometric exponents were 0.75, 0.94, 0.95 and 0.66 for CL, Vc, Vp and CLd, respectively. Fixing all the exponents increased the OFV to a value associated with a *P*-value of 0.07(LRT with 4 degrees of freedom). Individually fixed, the exponents of CL, Vc, Vp and CLd were associated with *P*-values of 1.00, 0.36, 0.13, 0.11, respectively, indicating that the exponents were not significantly different from the theoretical values. While a systematic underestimation persisted, there was a significant improvement in the prediction of woodchuck observations (Figure 4-4).

Low renal clearance of (−)-FTC and other nucleoside analogues in woodchucks has been reported.[18, 32,33] This fact is supported by the allometrically overestimated total clearance observed in the current analysis. This could ideally be tested by singling out a

renal clearance value for woodchuck as was done for total clearance. However, the scarcity of renal data did not allow for successful fitting of such a model to data. Renal and nonrenal clearance values (CLr and CLnr, respectively) obtained from fitting models to each species separately were used to estimate the allometric parameters by the two-stage method (log-log plots). Correlation coefficient for CLr was the low at 0.85, while it was 0.97 or higher for other parameters including CLnr. Removing woodchuck from the regression line enhanced the correlation for CLr radically to 1.0.

Although accounting for the low clearance of (−)-FTC in woodchuck enhanced the fit significantly, underpredicting woodchuck observations persisted, and all pharmacokinetic parameters were overestimated. To explore the scalability of woodchuck data in general, more flexibility was added for woodchuck data by introducing a new parameter (*c*) to the model as a multiplier of woodchuck body weight (Equation 4-4)

$$TVP_{ni} = a_n \, (c \, W_i)^{\,b_n} \qquad (4\text{-}4)$$

where (*c*) was allowed to be estimated (**model IV**). There was substantial enhancement in the prediction of woodchuck observations (Figure 4-5). OFV dropped significantly by 14.48 points, interindividual variability in CL dropped to 24%, and the estimates of allometric exponents were 0.784, 0.993, 1.00, 0.713 for CL, Vc, Vp and CLd, respectively, more closely in agreement and not significantly different than the theoretical values (associated with *P*-values of 0.39, 0.84, 0.83 and 0.53, respectively). Fixing all the exponents to their theoretical values increased the OFV to a value associated with a *P*-value of 0.27. As expected, the estimates of allometric exponents and coefficients are close to the values estimated without the woodchuck data. The estimate of woodchuck body weight multiplier was 0.59. A summary of all models is included in Table 4-2.

Discussion

There are instances in the literature where interspecies scaling based on body size predicted human pharmacokinetic properties with success.[34-36] It has been shown that allometric scaling of clearance is more successful for renally excreted and rapidly metabolized compounds, when elimination is dependent on physiological parameters (e.g. glomerular filtration rate and liver blood flow, respectively), which are known to scale allometrically.[37] On the other hand, for compounds where active transport processes are involved in the disposition, large unexplained interspecies differences can occur, and prediction of human pharmacokinetics based on allometry may well fail.[38] In addition, scaling pharmacokinetic properties based on total concentrations requires the assumption that protein binding is linear over the encountered range of concentrations, and similar across species. However, this is usually less important for compounds having low plasma protein binding.

Clinical pharmacokinetics of numerous nucleoside analogues have been successfully predicted based on studies in animal models.[39-43] Factors for this success include low and linear protein binding, highly efficient renal excretion, and little metabolism. Although the protein binding has not been characterized for (−)-FTC, it is assumed to be low and similar across species based on the experience with a myriad of other nucleoside analogues, including dideoxythiacytidine analogues.[39,43-47] Renal excretion of the unchanged compound was the predominant route of elimination for (−)-FTC in mice,[14] rats,[15,16] and rhesus[17] and cynomolgus monkeys.[14] Exceeding glomerular filtration rate and approaching renal plasma flow in rats, mice and monkeys, the clearance of (−)-FTC suggests active tubular secretion, and approaches renal plasma flow. [48,49] Since physiological processes like blood flows scale allometrically to the power of ¾,[21] it is expected that the clearance of (−)-FTC would scale to the same power. In addition, the volume of distribution at steady state of nucleoside analogues, including (−)-FTC, suggests distribution in total body water, which is consistent with

their low protein binding and hydrophilicity.[43] Anatomical volumes scale allometrically to the power of unity,[21] and hence the volumes of distribution of (−)-FTC are expected to scale to the same power. Indeed, both clearance (renal and nonrenal), and volumes of distribution of (−)-FTC scaled to the power values of ¾ and 1, respectively. The findings of this study further extend the power value of ¾ to distributional clearance scaling as well, a finding that has been scarcely reported in the literature.[29] Cosson et al[26] reported a power value of ~0.93 for the allometric relationship of distributional clearance. These findings augment the suggestion that the theoretical value of the allometric exponent may be a suitable alternative to an unconstrained estimate for describing species differences in clearance and distribution volume.[29] This practice is supported by empiricism as well as theory,[21,22] Nonetheless, special attention to specific dispositional properties for the compound in question; like differences between the species in modes of elimination, protein binding, dose proportionality, and low-efficiency active secretory or metabolic processes; remains an imperative for successful allometric scaling.

The observed deviation of renal and total clearances of (−)-FTC in woodchuck from the allometric relationship in the current analysis is supported by the reported low renal elimination of nucleoside analogues in woodchuck.[18, 32,33] Similar deviation from the allometric relationship for the total clearance of 3TC in woodchucks has been previously observed.[32,41] However, the volume of distribution of (−)-FTC in woodchucks was less deviant from the allometric relationship. Singling out woodchuck from the allometric relationship for CL and CLr enhanced the prediction of pharmacokinetic profiles for all species. However, deficiencies in predictions persisted. Serum concentrations of (−)-FTC in woodchuck were still systematically underpredicted after accounting for the outlying clearance, and all pharmacokinetic parameters were overestimated. Woodchucks are hibernating mammals, and experience circannual cycles of metabolic changes, and weight fluctuations that are almost entirely due to body fat content.[50] Since adipose tissue is not a clearing organ, and nucleoside analogues do not

distribute into fat due to their relatively hydrophilic nature, it is reasonable to suggest that body weight reported for woodchucks in this analysis has a higher fat fraction than other species, which needs to be adjusted for if woodchucks are to be included in the allometric relationship. Adipose tissue fraction in mice, rats and monkeys are similar (7-14%) and close to that of an average adult male human (13.6%),[51] meanwhile, lean body mass of woodchucks is hard to estimate, because the animals were housed in a 12 h light cycle, which could have affected the circannual cycle the animals normally undergo, and hence affect body weight and fat content. The addition of a woodchuck body weight multiplier to the model enhanced the fit tremendously, which suggests that the woodchuck is an allometric outlier, and suggests that a fraction of woodchuck body weight could place pharmacokinetic properties of woodchuck in the allometric relationship, save clearance. This fraction happened to be 0.56, which translates to close to 50% body fat, a reasonable value for woodchuck.[50] Assuming that underestimated body fat content was the underlying cause for woodchuck outlying allometric behavior, we are lead to the suggestion that body fat content needs to be accounted for in allometric scale-up by the use of lean rather than total body mass, or alternatively, animals of similar body fat content should be used for allometry.

The choice of the allometric model influenced the prediction of human pharmacokinetic parameters significantly (Table 4-2). After accounting for low clearance and the use of body weight multiplier for woodchuck, the predicted parameters in man were similar to those predicted by allometric scaling using data from mice, rats, and monkeys only. Closeness of these predictions to actual clinical pharmacokinetic parameters of (−)-FTC remains to be verified.

Allometric interspecies scaling of pharmacokinetic properties can be achieved in one step using nonlinear mixed effect modeling or nonlinear regression of superimposed Dedrick's plots, or in two by estimating the parameters in each species followed by linear regression of the log-log plots between the parameters and body weight. It has been

shown that the nonlinear mixed effects approach offers certain advantages over the other approaches.[52] This approach is able to deal with sparse and unbalanced data, frequently encountered in preclinical drug development, and to estimate all allometric parameters in one step. In addition, interindividual and residual error variability could be modeled with flexibility. Regression of superimposed Dedrick's plots assumes that the values of the allometric exponents are equal to their theoretical values of ¾ for clearances and 1 for volumes, and does not allow for their estimation. The criticism of the traditional two-stage approach addressing logarithmic transformations or the potential effect of data variability on regression statistics and the distortion of the slope of the allometric equation are avoided when nonlinear mixed effects modeling is used.[26]

In conclusion, the use of the knowledge base for a new chemical entity and the animal models it is tested in can better explain pharmacokinetic interspecies differences, which in turn may help predict human pharmacokinetics more accurately. Constraining the allometric exponents to their theoretical values may serve as a suitable alternative to an unconstrained estimate after special attention to dispositional properties and species differences in modes of elimination and protein binding. Success with other nucleoside analogues encourages the application of allometric scaling techniques to predict human pharmacokinetic properties to guide the choice of first human dose of new chemical entities in this, and possibly other, classes of compounds.

References

1. Doong S.-L., C.-H. Tsai, R. F. Schinazi, D. C. Liotta, and Y.-C. Cheng. 1991. Inhibition of the replication of hepatitis B virus *in vitro* by 2´,3´-dideoxy-3´-thiacytidine and related analogues. Proc. Natl. Acad. Sci. USA **88:**8495-8499.
2. Schinazi R. F., A. McMillan, D. Cannon, R. Mathis, R. M. Lloyd, A. Peck, J.-P. Sommadossi, M. St. Clair, J. Wilson, P. A. Furman, G. Painter, W.-B. Choi, and D. C. Liotta. 1992. Selective inhibition of human immunodeficiency viruses by

racemates and enantiomers of *cis*-5-fluoro-1-[2-(hydroxymethyl)-1,3-oxathiolan-5-yl]cytosine. Antimicrob. Agents Chemother. **36:**2423-2431.

3. Schinazi R. F., D. C. Liotta, W.-B. Choi, A. Peck, H. McClure, F. D. Boudinot, J.-P. Sommadossi, M. Davis, P. A. Furman, and G. Painter. 1992. Cellular pharmacology and monkey pharmacokinetics of the antiviral (−)-2′,3′-dideoxy-5-fluoro-3′-thiacytidine (FTC). National Collaborative Drug Discovery Group, Frontiers in HIV Therapy, San Diego, Calif., Nov. 3-7, p. 59.
4. Chang C.-N., S.-L. Doong, J. H. Zhou, J. W. Beach, L. S. Jeong, C. K. Chu, C. Tsai, and Y.-C. Cheng. 1992. Deoxycytidine deaminase-resistant stereoisomer is the active form of (±)-2′,3′-dideoxy-3′-thiacytidine in the inhibition of hepatitis B virus replication. J. Biol. Chem. **267:**13938-13942.
5. Schinazi R. F., C. K. Chu, A. Peck, A. McMillan, R. Mathis, D. Cannon, L. S. Jeong, J. W. Beach, W.-B. Choi, S. Yeola, and D. C. Liotta. 1992. Activities of the four optical isomers of 2′,3′-dideoxy-3′-thiacytidine (BCH-189) against human immunodeficiency virus type 1 in human lymphocytes. Antimicrob. Agents Chemother. **36:**672-676.
6. Soudeyns H., X.-J. Yao, Q. Gao, B. Belleau, J.L. Kraus, N. Nguyen-ba, B. Spira, and M. A. Wainberg. 1991. Anti-human immunodeficiency virus type 1 activity and in vitro toxicity of 2′-deoxy-3′-thiacytidine (BCH-189), a novel heterocyclic nucleoside analog. Antimicrob. Agents Chemother. **35:**1386-1390.
7. Furman P. A., M. Davis, D. C. Liotta, M. Paff, L. W. Frick, D. J. Nelson, R. E. Dornsife, J. A. Wurster, L. J. Wilson, J. A. Fyfe, J. V. Tuttle, W. H. Miller, L. Condreay, D. R. Averett, R. F. Schinazi, and G. R. Painter. 1992. The anti-hepatitis B virus activities, cytotoxicities, and anabolic profiles of the (−) and (+) enantiomers of *cis*-5-fluoro-1-[2-(hydroxymethyl)-1,3-oxathiolan-5-yl]cytosine. Antimicrob. Agents Chemother. **36:**2686-2692.

8. Cammack, N., P. Rouse, C. L. P. Marr, P. J. Reid, R. E. Boehme, A. V. Coates, C. R. Penn, and J. M. Cameron. 1992. Cellular metabolism of (−) enantiomeric 2´-deoxy-3´-thiacytidine. Biochem. Pharmacol. **43:**2059-2064.

9. Coates, J. A. V., N. Cammack, H. J. Jenkinson, I. M. Mutton, B. A. Pearson, R. Storer, J. M. Cameron, and C. R. Penn. 1992. The separated enantiomers of 2´-deoxy-3´-thiacytidine (BCH-189) both inhibit human immunodeficiency virus replication in vitro. Antimicrob. Agents Chemother. **36:**202-205.

10. Mathez, D., R. F. Schinazi, D. C. Liotta, and J. Leibowitch. 1993. Infectious amplification of wild-type human immunodeficiency virus from patients' lymphocytes and modulation by reverse transcriptase inhibitors in vitro. Antimicrob. Agents Chemother. **37:**2206-2211.

11. Hanna L. 1998. FTC: antiretroviral in development. Bulletin of Experimental Treatments for AIDS. July:38.

12. Pottage J., Thompson M., Kahn J., Delehanty J, McCreedy B., Rousseau F. Potent antiretroviral efficacy of low-dose FTC, initial results from a Phase I/II clinical trial. 5th Conference on Retroviruses and Opportunistic Infections. Chicago, IL. February 1998. Abstract 773.

13. Arasteh K; Muller M. 2001. New antiretroviral drugs. Improved pharmacokinetics and simpler dose schedules [Translated from German: Neue antiretrovirale Medikamente. Verbesserte Pharmakokinetik und Einfachere Dosierschemata]. MMW Fortschritte der Medizin. **143**(Suppl. 1):14-7.

14. Frick, L. W., C. U. Lambe, L. St. John, L. C. Taylor, and D. J. Nelson. 1994. Pharmacokinetics, oral bioavailability, and metabolism in mice and cynomolgus monkeys of (2´ *R*, 5´ *S*-)-*cis*-5-fluoro-1-[2-(hydroxymethyl)-1,3-oxathiolan-5-yl]cytosine, an agent active against human immunodeficiency virus and human hepatitis B virus. Antimicrob. Agents Chemother. **38**:2722-2729.

15. Frick, L. W., L. St. John, L. C. Taylor, G. R. Painter, P. A. Furman, D. C. Liotta, E. S. Furfine, and D. J. Nelson. 1993. Pharmacokinetics, oral bioavailability, and metabolic disposition in rats of (−)-*cis*-5-fluoro-1-[2-(hydroxymethyl)-1,3-oxathiolan-5-yl]cytosine, a nucleoside analog active against human immunodeficiency virus and hepatitis B virus. Antimicrob. Agents Chemother. **37:**2285-2292.

16. Abu-Raddad, E. J., D. C. Delinsky, M. G. Bartlett, M. J. Otto, R. F. Schinazi, D. B. Hall, F. D. Boudinot. Stereoselective Pharmacokinetics of 2´,3´-Dideoxy-5-Fluoro-3´-Thiacytidine in Rats. Submitted for publication.

17. Moore L.M., Ni L., Boudinot F.D., McClure H.M., and Schinazi R.F. The Pharmacokinetics of (−)-2',3'-Dideoxy-5-Fluoro-3'-Thiacytidine ((-)-FTC) and its Metabolites in Rhesus Monkeys. Submitted for publication.

18. Fox, L. M., M. A. Ascenzi, B. C. Tennant, J. Shi, R. F. Schinazi, and F. D. Boudinot. Stereoselective pharmacokinetics and metabolism of 2´-deoxy-5-fluoro-3´-thiacytidine (FTC) in woodchucks. Submitted for publication.

19. Reigner, B. G., P. E. O. Williams, I. H. Patel, J.-L. Steimer, C. Peck, and P. V. Brummelen. 1997. An evaluation of the integration of pharmacokinetic and pharmacodynamic principles in clinical drug development: Experience within Hoffmann-La Roche. Clin. Pharmcaokinet. **33**(2):142-152.

20. Mordenti, J. 1986. Man versus beast: Pharmacokinetic scaling in mammals. J. Pharm. Sci. **75**(11):1028.

21. Peters, R. H.1983. The ecological implications of body weight. Cambridge: Cambridge University Press.

22. West, G. B., J. H. Brown, B. J. Enquist. 1997. A general model for the origin of allometric scaling laws in biology. Science **276**:122-126.

23. Dedrick, R. L., Bischoff K. B., and Zaharko D. S. 1970. Interspecies correlation of plasma concentration history of methotrexate. Cancer Chemother. Rep. Part 1 **54**:95-101

24. Boxenbaum, H. 1982. Interspecies scaling, allometry, physiological time and the ground plan of pharmacokinetics. Journal of Pharmacokinetics and Biopharmaceutics. **10**(2):201-226.

25. Young, D., B. A. Patel, K. I. Plaisance, L. Augsburger, M. Ashraf, F. D. Boudinot, K. Doshi, J. M. Gallo, C. K. Chu, R. F. Schinazi, and McClure H. M. 1991. Application of NONMEM in allometric scaling. Pharmaceutical Research. **8**(10):S292.

26. Cosson, V. F., E. Fuseau, C. Efthymiopoulos, and A. Bye. 1997. Mixed effect modeling of sumatriptan pharmacokinetics during drug development. I: Interspecies allometric scaling. Journal of Pharmacokinetics and Biopharmaceutics. **25**(2):149-167.

27. Bies, R. R., H. C. Ko, R. Desjardins, J. Gobburu, C. C. Peck. 2000. Effective incorporation of preclinical information into the decision-making process for new drug development: An anonymous case study. Clinical Pharmacology and Therapeutics. **67**(2):107.

28. Bies R. R., H. C. Ko, J. Gobburu, E. Burak, B. Slusher, D. Hilt, J. Vornov, C. Bradley, C. Bradford, Sleczka B., W. Yang, C. Peck. 1999. Allometric scaling of pre-clinical pharmacokinetic data to predict human pharmacokinetic disposition for NAAL-1, a novel NAALADASE inhibitor. AAPS PharmSci. Vol. **1**, issue 4 (supplement).

29. Bies R. R., N. H. G. Holford, M. Karlsson, E. Burak, H. C. Kimko, C. C. Peck. 2000. A theoretical value of the allometric exponent may be a suitable alternative to an unconstrained estimate for describing species differences in distribution. AAPS PharmSci. Vol. **2**, issue 4 (supplement).

30. Beal, S. L., L. B. Sheiner (eds.). NONMEM Users Guides. NONMEM Project Group, University of California, San Francisco.

31. Rao, C. R. 1965. Linear statistical inference and its application. New York: John Wiley & Sons, pp. 347-52.

32. Rajagopalan, P., F. D. Boudinot, C. K. Chu, B. C. Tennant, B. H. Baldwin, and R. F. Schinazi. 1996. Pharmacokinetics of (−)-2′,3′-dideoxy-3′-thiacytidine in woodchucks. Antimicrob. Agents Chemother. **40**:642-645.

33. Witcher, J. W., F. D. Boudinot, B. H. Baldwin, M. A. Ascenzi, B. C. Tennant, J. F. Du, and C. K. Chu. 1997. Pharmacokinetics of 1-(2-fluoro-5-methyl-β-L-arabinofuranosyl)-uracil (L-FMAU) in woodchucks. Antimicrob. Agents Chemother. **41**:2184-2187.

34. Paxton, J. W., D. Young, I. G. G. Robertson. 1993. Pharmacokinetics of acridine-4-carboxamide in the rat, with extrapolation to humans. Cancer Chemother. Pharmacol. **32**(4): 323-5

35. Cruze, C. A., G. R. Kelm, and M. P. Meredith. 1995. Interspecies scaling of tebufelone pharmacokinetics data and application to preclinical toxicology. Pharm. Res. **12**(6):895-901.

36. Lave, T., A. H. Schmitt-Hoffmann, P. Coassolo, B. Valles, G. Ubeaud, B. Ba, R. Brandt, R. C. Chou. 1995. A new extrapolation method from animals to man: application to a metabolized compound, mofarotene. Life Sci. **56**(26):PL473-8.

37. Boxenbaum B., R. W. D'Souza. 1990. Inter-species pharmacokinetic scaling, biological design and neoteny. In: Testa B. (Ed.) Advances in Drug Research, Academic Press, London, p. 139-196.

38. Lave T., Portmann R., Schenker G., Gianni A., Guenzi A., Girometta M.-A., and Schmitt M. 1998. Interspecies pharmacokinetic comparisons and allometric scaling of napsagatran, a low molecular weight thrombin inhibitor. Journal of Pharmacy and Pharmacology. **51**:85-91.

39. Ibrahim S. S., and F. D. Boudinot. 1989. Pharmacokinetics of 2',3'-dideocycytidine in rats: application to interspecies scale-up. Journal of Pharmacy and Pharmacology **41**:829-834.

40. Patel B. A., F. D. Boudinot, R. F. Schinazi, J. M. Gallo, and C. K. Chu. 1990. Comparative pharmacokinetics and interspecies scaling of 3'-azido-3'-deoxythymidine (AZT) in several mammalian species. Journal of Pharmacobio-Dynamics. **13**:206-211.

41. Simmons, P. T., F. D. Boudinot. Application of interspecies scale up for initial clinical trials of nucleoside analogs. Submitted for publication.

42. Hussey E. K., K. H. Donn, M. J. Daniel, S. T. Hall, A. J. Harker, and G. L. Evans. 1994. Interspecies scaling and pharmacokinetic parameters of 3TC in humans. Journal of Clinical Pharmacology. **34**:975-977.

43. Kaul, S., K. A. Dandekar, B. E. Schillin, and R. H. Barbhaiya. 1999. Toxicokinetics of 2',3'-didehydro-3'-deoxythymidine, Stavudine (D4T). Drug Metabolism and Disposition. **27**(1):1-12.

44. Perry, C. M., D. Faulds. 1997. Lamivudine: A review of its antiviral activity, pharmacokinetic properties and therapeutic efficacy in the management of HIV infection. Drugs. **53**:657-680.

45. Retrovir® (Zidovudine; AZT) product information. GlaxoSmithKline Inc., Research Triangle Park, NC.

46. Collins, J. M., R. W. Klecker, J. A. Kelly, J. S. Toth, C. L. McCully, F. M. Balis, and D. G. Poplack. 1988. Pyrimidine dideoxyribonucleosides: Selectivity of penetration into cerebrospinal fluid. The Journal of Pharmacology and Experimental Therapeutics. **245**:466-470.

47. Brog, N., and L. Stahle. 1998. Pharmacokinetics and distribution over the blood-brain barrier of Zalcitabine (2',3'-dideoxycytidine) and BEA005 (2',3'-dideoxy-

3’-hydroxymethylcytidine) in rats, studied by microdialysis. Antimicrobial agents and Chemotherapy. **42**(9):2174-2177.

48. Holt, J. P., and E. A. Rhode. 1976. Similarity of renal hemodynamics in mammals. Am. Heart J. 92:465-472.
49. Gerlowski, L. E., and R. K. Jain. 1983. Physiologically based pharmacokinetic modeling: Principles and applications. Journal of Pharmaceutical Sciences. 72(10):1103-1127.
50. Davis D. E. 1967. The annual rhythm of fat deposition in woodchucks (*Marmota monax*). Physiol. Zool. **40**:391-402.
51. Brown, R. P., M. D. Delp, S. L Lindtedt, L. R. Rhomberg, and R. P. Beliles. 1997. Physiological parameter values for physiologically based pharmacokinetic models. Toxicology and Industrial Health. **13**(4):407-484.
52. Efthymiopoulos, C., V. Cosson, and A. Bye. The use of NONMEM in the interspecies allometric scaling (Abstract). Second meeting of Page, London, June 1994.

Table 4-1. Summary of collected data and pharmacokinetic parameters for each species.

Parameter	**Mouse**	**Rat**	**Woodchuck**	**Monkey**
Reference	14	16	18	17
Dose (mg/kg)	10	19 – 51	20	33.3
	100			
	600			
No. of animals	34	10	3	3
No. of observation per animal (average)	1	8.8	11	10
Average body weight W (kg)	0.035	0.295	4.67	4.48
Total clearance CL (L/h)	0.0663	0.464	1.01	2.85
Renal clearance CLr (L/h)	0.0579	0.281	0.303	1.64
Nonrenal clearance CLnr (L/h)	0.00841	0.183	0.704	1.44
Central compartment volume Vc (L)	0.0240	0.207	1.23	1.91
Peripheral compartment volume Vp (L)	0.00760	0.191	1.89	2.43
Distributional clearance CLd (L/h)	0.00470	0.369	2.54	2.73

Table 4-2. Summary of allometric mixed effects models fit to the data. See text for details.

Model	Description	OFV	LLD (*P*-value)	Structural parameter estimates (95% confidence interval)				Interindividual variability	Prediction in man
				Coefficients		Exponents		(CV%)	(70-kg)
I	$TVCL = a_1 W^{b1}$	236.257		a_1	0.74	b_1	0.69	37	13.8
	$TVVc = a_2 W^{b2}$			a_2	0.41	b_2	0.93	25	28.7
	$TVVp = a_3 W^{b3}$			a_3	0.52	b_3	0.94	15	21.2
	$TVCLd = a_4 W^{b4}$			a_4	1.01	b_4	0.65	3.5	15.9
II	$TVCL = a_1 W^{b1}$	162.389		a_1	1.02	b_1	0.79	20	29.3
	$TVVc = a_2 W^{b2}$			a_2	0.50	b_2	1.02	16	42.2
	$TVVp = a_3 W^{b3}$			a_3	0.57	b_3	1.01	12	38.5
	$TVCLd = a_4 W^{b4}$			a_4	1.03	b_4	0.69	14	19.5
	(no woodchuck data)								

Table 4-2 (Cont'd). Summary of allometric mixed effects models fit to the data. See text for details.

Model	Description	OFV	LLD (*P*-value)	Structural parameter estimates (95% confidence interval)				Interindividual variability	Prediction in man
				Coefficients		Exponents		(CV%)	(70-kg)
III	$TVCL_{woodchuck} = a_0$	217.843	18.414 †	a_0	1.38				
	$TVCL = a_1 W^{b1}$		($P < 0.0001$)	a_1	0.89	b_1	0.75	26	21.3
	$TVVc = a_2 W^{b2}$			a_2	0.40	b_2	0.94	33	28.3
	$TVVp = a_3 W^{b3}$			a_3	0.50	b_3	0.95	20	22.1
	$TVCLd = a_4 W^{b4}$			a_4	0.99	b_4	0.66	8.1	16.0
IV ¥	$TVCL_{woodchuck} = a_0$	203.365	14.48 §	a_0	1.11				
	$TVCL = a_1 (cW)^{b1}$		($P = 0.0001$)	a_1	0.99	b_1	0.78	24	27.7
	$TVVc = a_2 (cW)^{b2}$			a_2	0.48	b_2	0.99	27	40.3
	$TVVp = a_3 (cW)^{b3}$			a_3	0.57	b_3	1.00	16	32.8
	$TVCLd = a_4 (cW)^{b4}$			a_4	1.04	b_4	0.71	12	21.5

† Compared to **model I**.

§ Compared to **model III**.

¥ The body weight multiplier (c) has a value of 1 for mouse, rat and monkey, and was allowed to be estimated for woodchuck.

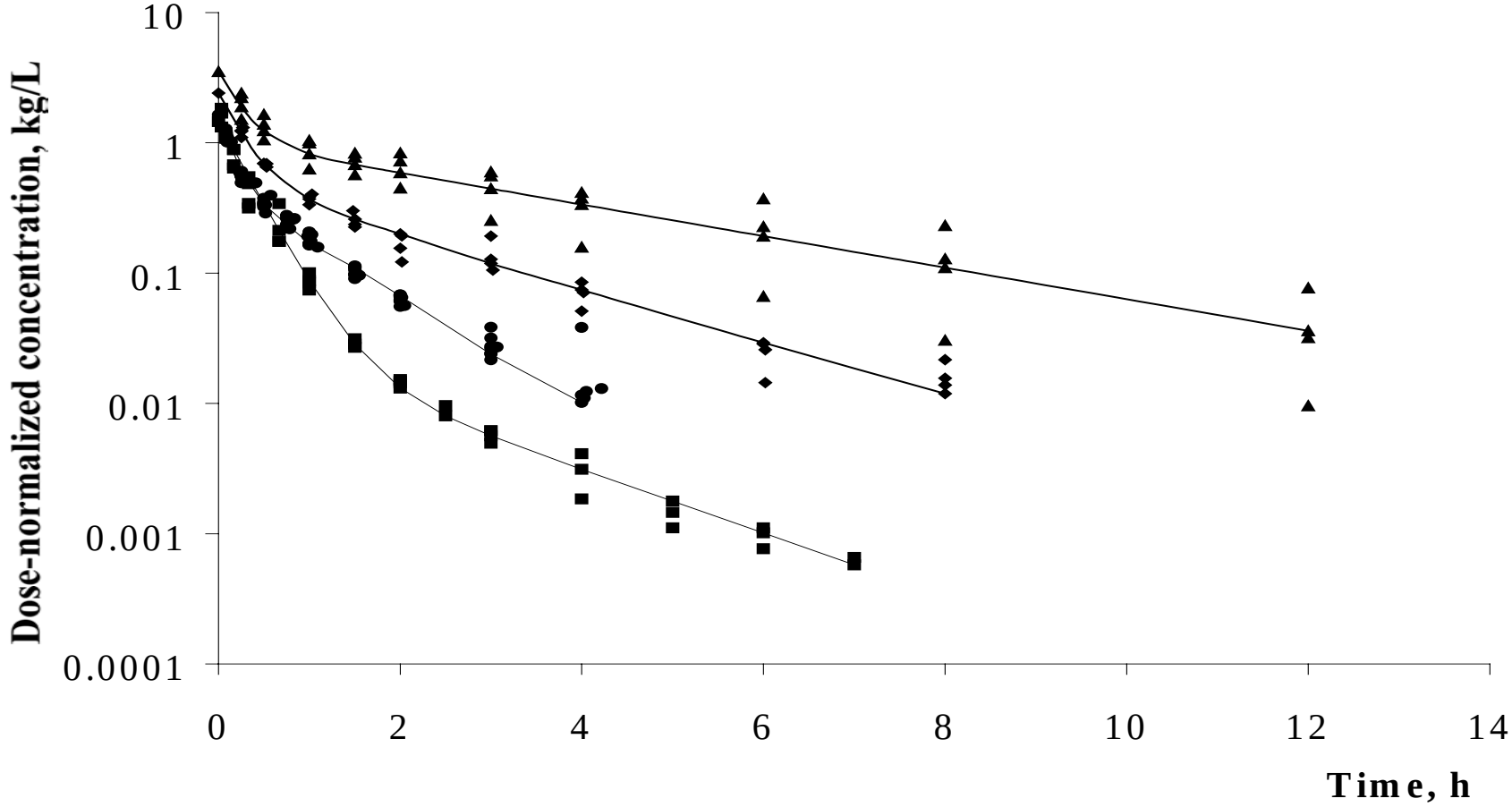

Figure 4-1. Intravenous observed (symbols) and model-predicted (lines) FTC profiles in mice (■), rats (●), woodchucks (▲), and rhesus monkeys (♦).

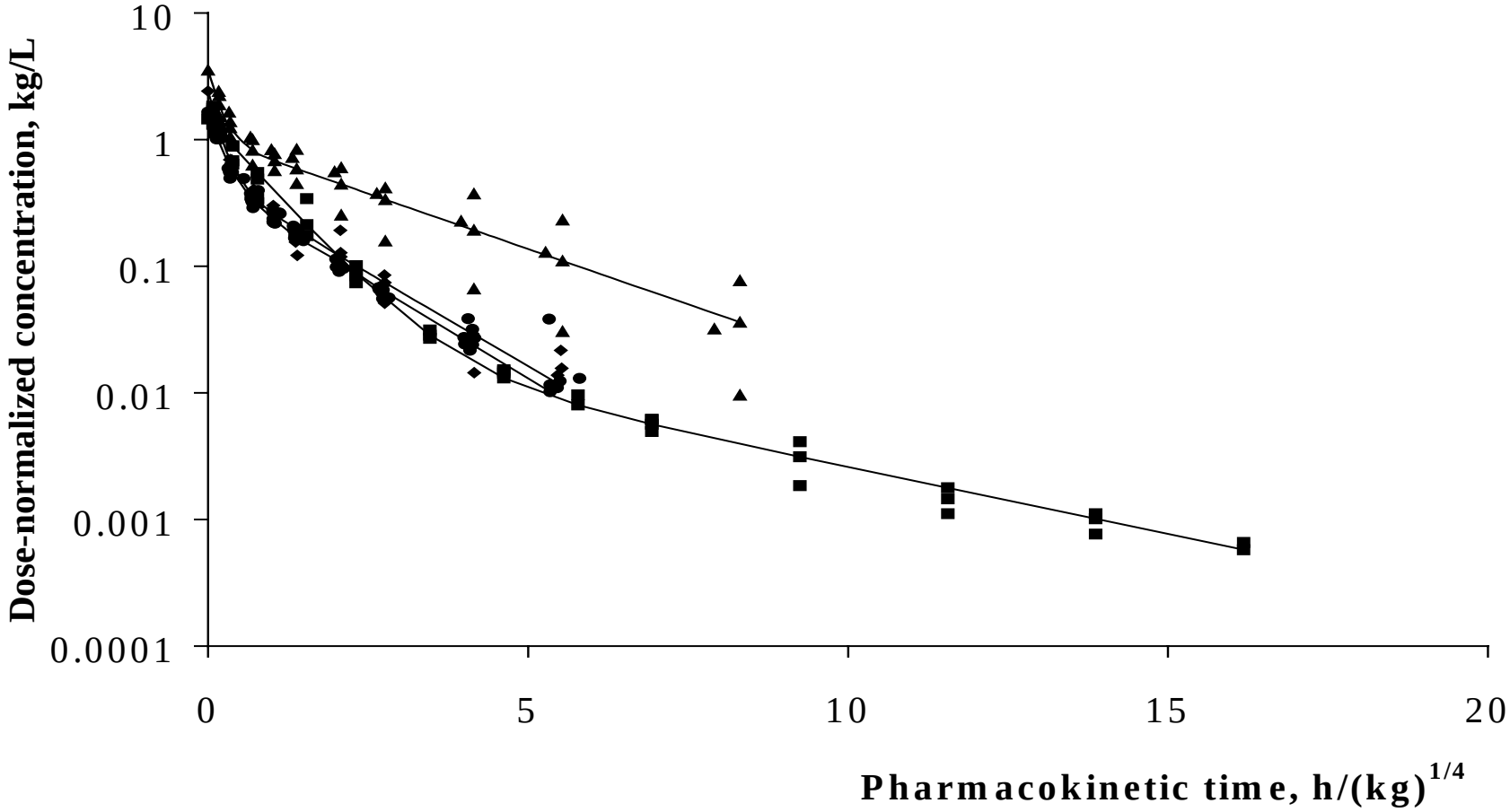

Figure 4-2. Elementary Dedrick's plot for observed (symbols) and predicted (lines) FTC profiles in mice (■), rats (●), woodchucks (▲), and rhesus monkeys (♦).

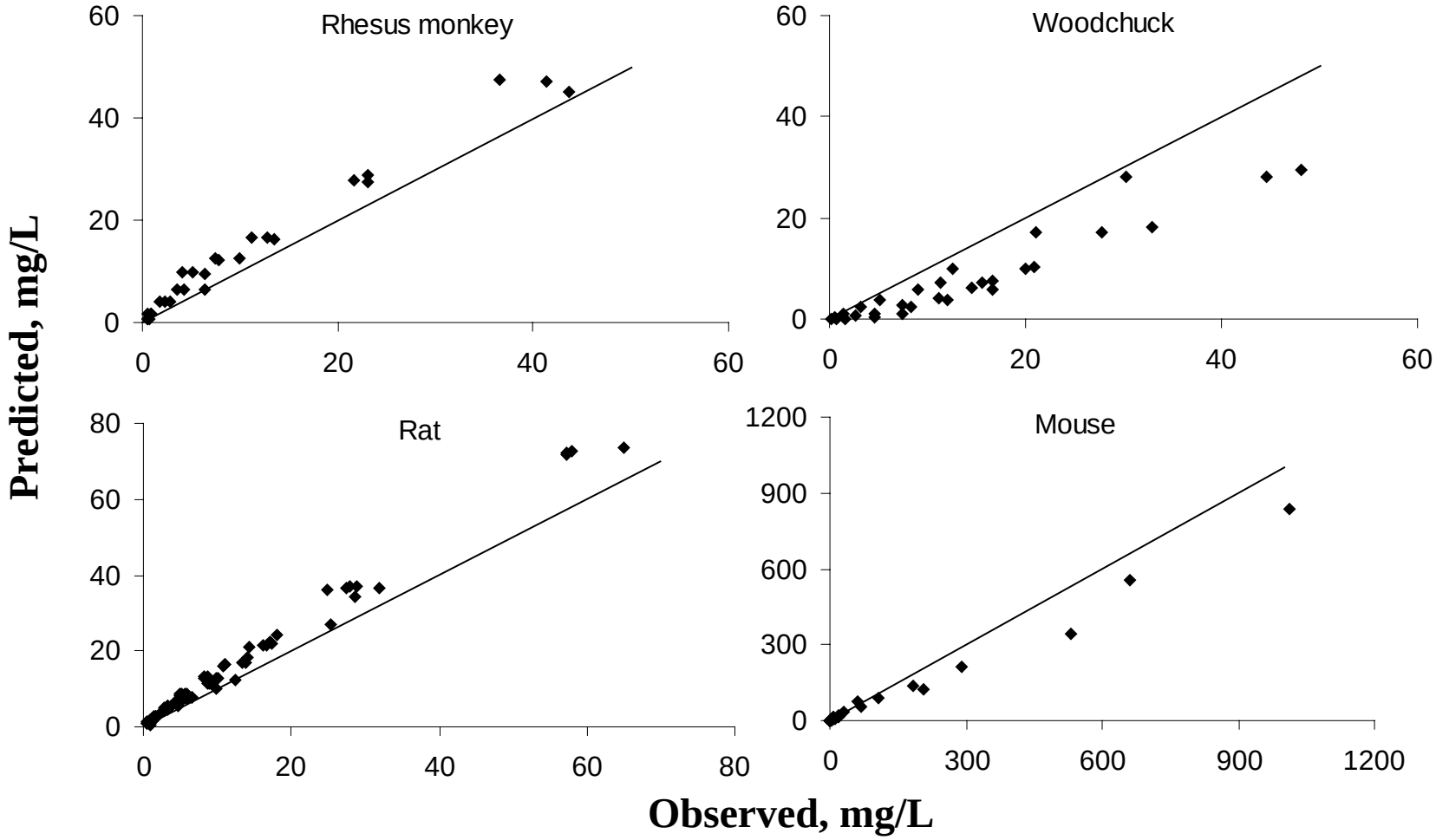

Figure 4-3. Concentrations (mg/L) predicted by **model I** *vs*. concentrations (mg/L) observed.

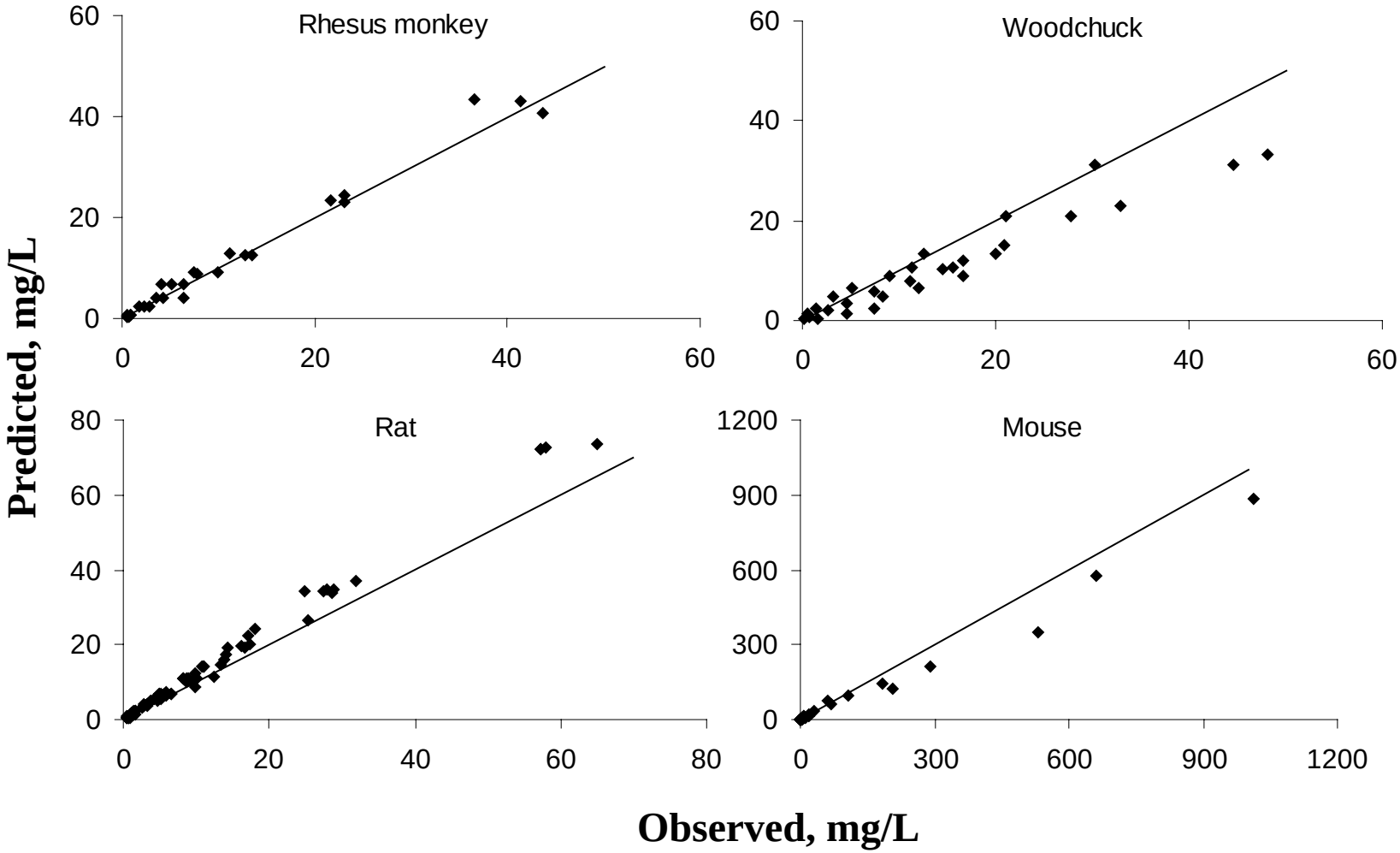

Figure 4-4. Concentrations (mg/L) predicted by **model III** *vs*. concentrations (mg/L) observed.

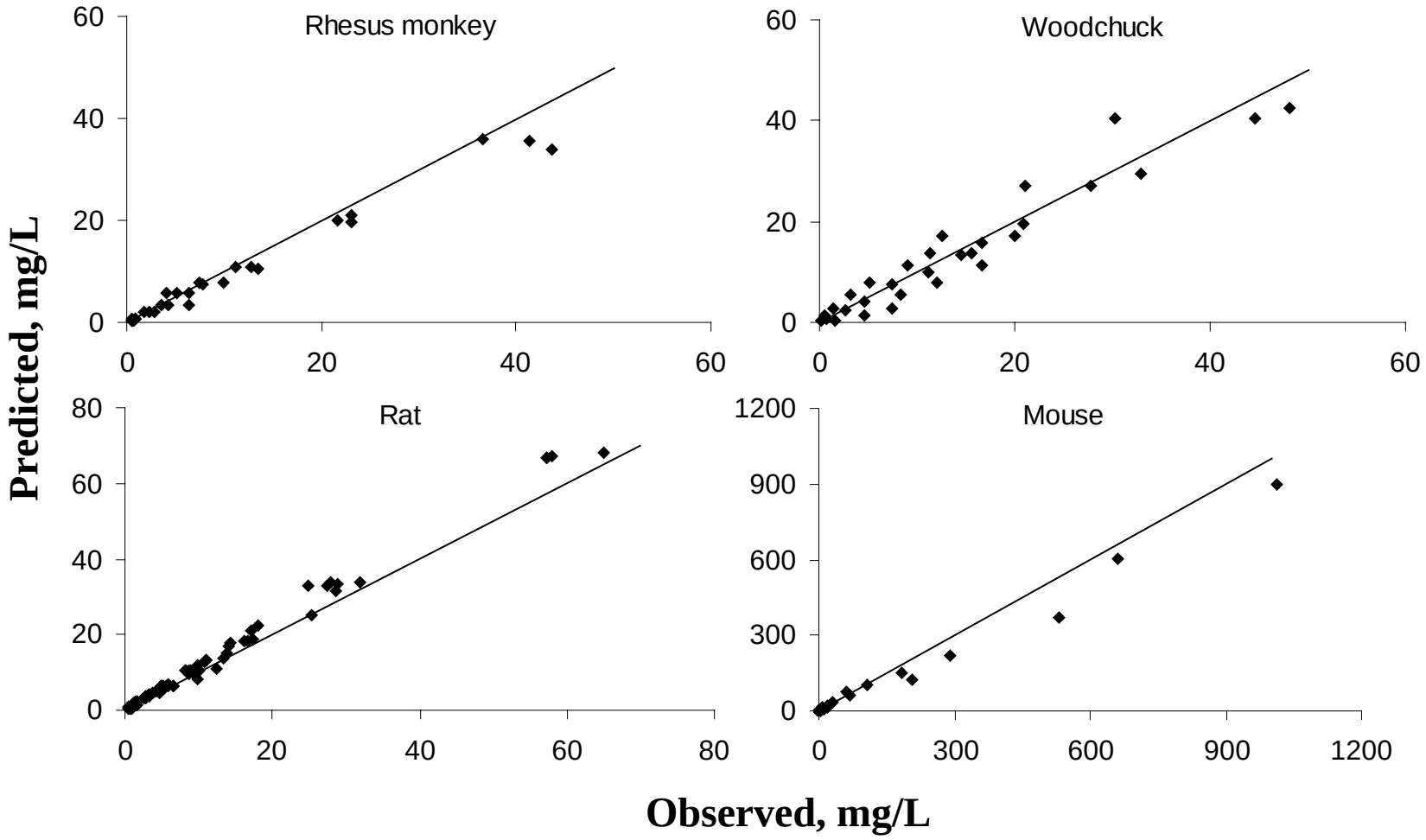

Figure 4-5. Concentrations (mg/L) predicted by **model IV** *vs*. concentrations (mg/L) observed.

CHAPTER 5

CONCLUSIONS

The search for safe and effective therapeutic agents for the treatment of infections caused by invading organisms continues to be of paramount importance. Analogues of nucleic bases and nucleosides have offered an arsenal of agents in the battle between man and invading organisms. HIV, HBV, and fungal infections are among conditions these analogues have been of value.

Pharmacokinetics of 4-azido-5-fluoro-2(1H)-pyrimidinone and 5-fluorocytosine in rats

The use of the cytosine analogue flucytosine (5-FC) has been limited by bone marrow and liver toxicities encountered at high concentrations.[1] In an effort to overcome the toxicity of 5-FC at high concentrations, a prodrug might offer a dampening effect on the higher concentrations, and prolong the half life of the drug. 4-Azido-5-fluoro-2(1H)-pyrimidinone (A-5-FP) has been synthesized as a potential prodrug for 5-FC. It was hypothesized that a reductase enzyme system analogous to the reductase acting on the azido-purine analogues would catalyze the conversion of the azido-pyrimidine A-5-FP to 5-FC.

Contrary to the hypothesis, 5-FC was not detected in plasma or urine after administering A-5-FP to rats. 5-Fluorouracil was not detected in plasma or urine, either. Combined with the fact that 5-FC and 5-FU are appreciably excreted in the urine,[2,3] we conclude that unlike the case with azido-purine analogues, a catalytic enzyme that would reduce the azide group in the azido-pyrimidine analogue A-5-FP is probably absent. Whether this is true for all azido-pyrimidine analogues is to be verified. On the other

hand, the disposition of A-5-FP was quite different from 5-FC in some aspects. Biexponential decline was observed for both A-5-FP and 5-FC. Meanwhile, A-5-FP distributed slower than 5-FC, and had higher renal and nonrenal clearances. Distribution volume of A-5-FP was similar to that of 5-FC and consistent with values obtained for other nucleoside analogues.

The dispositional and metabolic profile of A-5-FP deems it unfavorable for development as a prodrug of 5-FC.

Stereoselective pharmacokinetics of 2´,3´-dideoxy-5-fluoro-3´-thiacytidine in rats

2´,3´-Dideoxy-5-fluoro-3´-thiacytidine, (RCV, Racivir™) has shown high activity against HIV and HBV. The S-(−) enantiomers of RCV, emtricitabine ((−)-FTC; Coviracil®), corresponding to the unnatural L form, possess greater antiviral activity in cultured cells than the corresponding R-(+) enantiomers. Pharmacokinetic differences between the enantiomers of RCV have been reported in woodchuck.[4] However, due to the absence an enantioselective analytical methodology, the characterization of stereoselective pharmacokinetics of RCV was still lacking answers to specific questions regarding chiral inversion and enantiomer-enantiomer interactions.

The enantiomers of RCV were separated and quantified using a chiral capillary electrophoretic method with hydroxypropyl-β-cyclodextrin as the chiral media. The method proved linear, selective, precise and accurate over the range of 0.5-100 µg/ml for both enantiomers. The method managed to separate the enantiomer of RCV from a potential metabolite (FTU). This was the first chiral method for the determination of enantiomers of RCV in biological matrices.

Chiral inversion was ruled out for both enantiomers in rats. This result is supported by similar result for (−)-FTC in rhesus monkeys. In addition, plasma profiles were visibly comparable for the two enantiomers. The (+)-enantiomer showed higher

renal and nonrenal clearances, and faster more complete absorption than the (−)-enantiomer. Initial distribution volume for the (+)-enantiomer was larger as well.

Enantiomer-enantiomer interactions were detected, reducing steady-state distribution volume, and slowing absorption for both enantiomers. The effect of (+)-FTC on (−)-FTC was less profound than that of (−)-FTC on (+)-FTC.

In general, the pharmacokinetics of RCV was characterized by slight to moderate stereoselectivity and weak enantiomeric interaction. In view of much higher activity of (−)-FTC against HBV and HIV compared to (+)-FTC, these findings may offer to support the development of the racemic mixture as a less expensive alternative to pure (−)-FTC.

Allometric interspecies scaling of (−)-2´,3´-dideoxy-5-fluoro-3´-thiacytidine

Establishing allometric relationship has traditionally been conducted by obtaining pharmacokinetic parameters for multiple species using noncompartmental analysis methods, followed by linear regression of log-transformed parameters on log-transformed body weight. Although simple and easy to implement, this 2-stage approach suffers from limitations addressing logarithmic transformations and the potential effect of data variability on regression statistics and the distortion of the slope of the allometric equation.

An alternative approach to the 2-stage method is to conduct nonlinear regression on superimposed Dedrick's plots. These plots are constructed by transforming plasma concentrations and time axes based on the theoretical values of ¾ and 1 for the allometric exponents of clearances and volumes. Although predictive of plasma profiles in different species, this approach alone cannot deal with the case when the exponents are different than the theoretical values, unless combined with the 2-stage approach.

Nonlinear mixed effects modeling (NONMEM) has recently been used to characterize allometric dependence of pharmacokinetic properties.[5-9] The ability to obtain allometric coefficients and exponents in a single step, and the flexibility of adding

more complicated covariate and statistical structures, make NONMEM a more plausible approach. The limitations of the previous approaches are avoided with NONMEM.

Allometric scaling has been proven successful for a number of nucleoside analogues. Advantageous properties like low protein binding, and renal elimination, enhanced the scalability of the pharmacokinetics of nucleoside analogues. Indeed, this success has set an encouraging tone for allometric scaling as a prospective predictive tool for the development of new nucleoside analogues.

The allometric scaling of dispositional properties of (−)-FTC in four species, namely mice, rats, woodchucks and rhesus monkeys, was attempted. Nonlinear mixed effects modeling was used to achieve that purpose. The difference between woodchuck and other species in clearance was accounted for. In addition, more flexibility was added for woodchuck by introducing an estimable body weight multiplier.

Accounting for specific differences, and using the allometric model to scale dispositional properties resulted in accurately predicting pharmacokinetic profiles of (−)-FTC in the species used in model building. Pharmacokinetic parameters were predicted for a normal 70-kg man based on the developed allometric relationship, and awaits verification from current clinical studies.

The allometric exponents were in close agreement with and not significantly different from empirically and theoretically suggested values of ¾ for clearances and 1 for volumes.[10,11] This is in support of the recent theory and model developed in an attempt to explain the quarter-power law.

Summary

Azido-pyrimidine analogues may not be suitable prodrugs for their amino-counterparts. RCV exhibits enantioselective absorption and disposition in rats. The magnitude of difference is not as profound as what was seen in woodchucks, mainly due to the absence of fast and extensive deamination of (+)-FTC in rats lacking deaminase

activity. No chiral inversion was observed, and a weak interaction between the enantiomers was seen in absorption rate and volumes of distribution. Finally, due to greater flexibility, NONMEM offers a plausible approach for allometric pharmacokinetic scaling. Interspecies differences in the pharmacokinetics of (−)-FTC were explained by body weight according to the allometric equation after accounting for low clearance and higher body fat content in woodchuck.

Reference

1. Bennett J. E. 1990. Antifungal agents. In: Goodman and Gillman: The Pharmacological Basis of Therapeutics. McGraw-Hill, New York, NY. pp. 1168-1169.
2. Koechlin BA, Rubio F, Palmer S, Gabriel T, Duschinsky R. The metabolism of 5-fluorocytosine-2^{14}C and of cytosine-^{14}C in the rat and the disposition of 5-fluorocytosine-2^{14}C in man. *Biochemical Pharmacology* 1966, **15**: 435-446.
3. Jarugula VR, Lam SS, Boudinot FD. Nonlinear pharmacokinetics of 5-fluorouracil in rats. *J Pharm Sci* 1997, **86**: 756-758.
4. Fox, L. M., M. A. Ascenzi, B. C. Tennant, J. Shi, R. F. Schinazi, and F. D. Boudinot. Stereoselective pharmacokinetics and metabolism of 2´-deoxy-5-fluoro-3´-thiacytidine (FTC) in woodchucks. Submitted for publication.
5. Young, D., B. A. Patel, K. I. Plaisance, L. Augsburger, M. Ashraf, F. D. Boudinot, K. Doshi, J. M. Gallo, C. K. Chu, R. F. Schinazi, and McClure H. M. 1991. Application of NONMEM in allometric scaling. Pharmaceutical Research. **8**(10):S292.
6. Cosson, V. F., E. Fuseau, C. Efthymiopoulos, and A. Bye. 1997. Mixed effect modeling of sumatriptan pharmacokinetics during drug development. I: Interspecies allometric scaling. Journal of Pharmacokinetics and Biopharmaceutics. **25**(2):149-167.

7. Bies, R. R., H. C. Ko, R. Desjardins, J. Gobburu, C. C. Peck. 2000. Effective incorporation of preclinical information into the decision-making process for new drug development: An anonymous case study. Clinical Pharmacology and Therapeutics. **67**(2):107.
8. Bies R. R., H. C. Ko, J. Gobburu, E. Burak, B. Slusher, D. Hilt, J. Vornov, C. Bradley, C. Bradford, Sleczka B., W. Yang, C. Peck. 1999. Allometric scaling of pre-clinical pharmacokinetic data to predict human pharmacokinetic disposition for NAAL-1, a novel NAALADASE inhibitor. AAPS PharmSci. Vol. **1**, issue 4 (supplement).
9. Bies R. R., N. H. G. Holford, M. Karlsson, E. Burak, H. C. Kimko, C. C. Peck. 2000. A theoretical value of the allometric exponent may be a suitable alternative to an unconstrained estimate for describing species differences in distribution. AAPS PharmSci. Vol. **2**, issue 4 (supplement).
10. West, G. B., J. H. Brown, and B. J. Enquist. 1997. A general model for the origin of allometric scaling laws in biology. Science. **276**:122-126.
11. Peters, R. H. The Ecological Implications of Body Size. Cambridge University Press, NewYork, NY. 1983.

APPENDIX A

NONMEM INPUT FILE DESCRIBING A 2-COMPARTMENT MODEL

The following control stream includes a representative NONMEM input file describing the 2-compartment model used to fit the data of each of the four groups obtained after administering RCV and its enantiomers to rats. See chapter 3 for details.

```
$PROBLEM        STEREOSELECTIVE PK OF RCV IN RATS, 2-CMT
$INPUT       ID PERI TRT ENT FORM TIME AMT=DOSE WGT EVID CMT DV
$DATA        PP.DAT IGNORE=C
$SUBROUTINES  ADVAN4 TRANS4  ;CL V2 V3 KA  Q
$PK

TVCL=THETA(1)
CL=TVCL
TVV2=(THETA(2))
V2=TVV2
TVV3=(THETA(3))
V3=TVV3
TVQ=THETA(4)
Q=TVQ
TVF0=(THETA(5))
F0=TVF0
TVKA=(THETA(6))
KA=TVKA*EXP(ETA(1))
TVF1=(THETA(7))
F1=TVF1

SC=V2
S0=1

$ERROR

YP=F*(1+ERR(1))+ERR(2)          ;FOR PLASMA OBSERVATIONS
YU=F+ERR(3)                     ;FOR URINE OBSERVATIONS
```

```
SW=0
IF(CMT.EQ.2) SW=1
Y=(SW*YP)+((1-SW)*YU)

IPRED=F
IRES=DV-IPRED

$THETA  (0,.651)          ;1 CL
$THETA  (0,.36)           ;2 V2
$THETA  (0,.105)          ;3 V3
$THETA  (0,.208)          ;4 Q
$THETA  (0,.523,1)        ;5 FRACTION IN URINE
$THETA  (0,.703)          ;6 KA
$THETA  (0,.809,1)        ;7 BIOAVAILABILITY

$OMEGA .1

$SIGMA  .03 .1 1.4

$ESTIMATION       METHOD=1 NOABORT MAXEVAL=9000 PRINT=2
                  SIGDIGITS=3 INTERACTION POSTHOC

$COVARIANCE
```

APPENDIX B

NONMEM INPUT FILE FOR TESTING HYPOTHESES REGARDING STEREOSELECTIVE PHARMACOKINETICS OF RACIVIR

The following control stream includes a representative NONMEM input file describing the model used for testing the hypotheses regarding stereoselectivity and enantiomer-enantiomer interactions for RCV. See chapter 3 for details.

```
.
$PROBLEM STEREOSELECTIVE PK OF RCV IN RATS, HYPOTHESIS TESTING

$INPUT       ID PERI TRT ENT FORM TIME AMT=DOSE WGT EVID CMT DV
;TRT=1 for PLS after PLS
;TRT=2 for PLS after RAC
;TRT=3 for MNS after MNS
;TRT=4 for MNS after RAC

$DATA        ORAL-8$.DAT IGNORE=C

$SUBROUTINES  ADVAN4 TRANS4
$PK
X1=-1
X2=0
X3=0

IF (TRT.EQ.1) THEN
X1=1
X2=1
ENDIF

IF (TRT.EQ.2) THEN
X1=1
X2=-1
ENDIF

IF (TRT.EQ.3) X3=1

IF (TRT.EQ.4) X3=-1
```

```
TVCL=THETA(1)+(THETA(8)*(X1))+(THETA(15)*(X2))+(THETA(21)*(X3))
CL=TVCL*EXP(ETA(1))

TVV2=(THETA(2))+(THETA(9)*(X1))+(THETA(16)*(X2))+(THETA(22)*(X3))
V2=TVV2

TVV3=(THETA(3))+(THETA(10)*(X1))+(THETA(17)*(X2))+(THETA(23)*(X3))
V3=TVV3

TVF0=(THETA(5))+(THETA(12)*(X1))+(THETA(18)*(X2))+(THETA(24)*(X3))
F0=TVF0

TVKA=(THETA(6))+(THETA(13)*(X1))+(THETA(19)*(X2))+(THETA(25)*(X3))
KA=TVKA*EXP(ETA(2))
TVF1=(THETA(7))+(THETA(14)*(X1))+(THETA(20)*(X2))+(THETA(26)*(X3))
F1=TVF1*EXP(ETA(3))

IF (TRT.EQ.1) TVQ=THETA(4)
IF (TRT.EQ.2) TVQ=THETA(4)
IF (TRT.EQ.3) TVQ=THETA(11)
IF (TRT.EQ.4) TVQ=THETA(11)
Q=TVQ

SC=V2
S0=1

$ERROR
YP=F*(1+ERR(1))+ERR(2)          ;FOR PLASMA OBSERVATIONS
YU=F+ERR(3)                     ;FOR URINE OBSERVATIONS
SW=0
IF(CMT.EQ.2) SW=1
Y=(SW*YP)+((1-SW)*YU)

IPRED=F
IRES=DV-IPRED

$THETA  (0,.537)        ;1 CL
$THETA  (0,.26)         ;2 V2
$THETA  (0,.129)        ;3 V3
$THETA  (0,.377)        ;4 Q (PLS)
$THETA  (0,.595,1)      ;5 FRACTION IN URINE
$THETA  (0,.52)         ;6 KA
$THETA  (0,.764,1)      ;7 BIOAVAILABILITY
```

```
$THETA  (.0839)          ;8 CL  pp+pr=mm+mr
$THETA  (.0342)          ;9 V2  pp+pr=mm+mr
$THETA  (-.00763)        ;10 V3  pp+pr=mm+mr
$THETA  (0,.296)         ;11  Q (MNS)
$THETA  (-.0499)         ;12 F0  pp+pr=mm+mr
$THETA  (.0568)          ;13 KA  pp+pr=mm+mr
$THETA  (0.068)          ;14 F   pp+pr=mm+mr

$THETA  (.03441)         ;15 CL  pp=pr
$THETA  (.0501)          ;16 V2  pp=pr
$THETA  (.00468)         ;17 V3  pp=pr
$THETA  (-.0327)         ;18 F0  pp=pr
$THETA  (.0851)          ;19 KA  pp=pr
$THETA  (.009141)        ;20 F   pp=pr

$THETA  (.00766)         ;21 CL  mm=mr
$THETA  (.0089)          ;22 V2  mm=mr
$THETA  (.0117)          ;23 V3  mm=mr
$THETA  (.0661)          ;24 F0  mm=mr
$THETA  (.0761)          ;25 KA  mm=mr
$THETA  (-.0414)         ;26 F   mm=mr

$OMEGA .000264 .0296 .00464

$SIGMA  .018 .085 1.2

$ESTIMATION METHOD=1 NOABORT MAXEVAL=9000 PRINT=2 SIGDIGITS=3
                    INTERACTION POSTHOC

$COVARIANCE
```

APPENDIX C

NONMEM INPUT FILE FOR ALLOMETRIC SCALING

The following control stream includes a NONMEM input file describing **model III** in chapter 4 where pharmacokinetic allometric scaling was applied to data for (−)-FTC obtained from monkeys, woodchucks, rats and mice, and (−)-FTC clearance in woodchuck was singled out of the allometric relationship and allowed to be estimated. See chapter 4 for details.

```
$PROBLEM   INTERSPECIES SCALING OF (−)-FTC

$INPUT     CPD SPC ID BW DSKG DOSE=AMT DSML ROUT
           EVID CMT TIME OBS=DV OBML
;SPC=1 for rhesus monkeys
;SPC=2 for woodchucks
;SPC=3 for rats
;SPC=4 for mice

$DATA      FTCSCALEIVNOURINE.DAT IGNORE=C

$SUBROUTINES  ADVAN3 TRANS4

$PK
IF (SPC.EQ.2) THEN
TVCL=THETA(9)
ELSE
TVCL=THETA(1)*BW**THETA(2)
ENDIF
TVV1=THETA(3)*BW**THETA(4)
TVV2=THETA(5)*BW**THETA(6)
TVQ=THETA(7)*BW**THETA(8)

CL=TVCL*EXP(ETA(1))
V1=TVV1*EXP(ETA(2))
V2=TVV2*EXP(ETA(3))
Q=TVQ*EXP(ETA(4))
```

```
SC=V1

$ERROR

IPRED=F
IRES=DV-IPRED
Y=F*(1+ERR(1))+ERR(2)

$THETA  (0,.901)          ;1 CL COEFFICIENT
$THETA  0.745             ;2 CL EXPONENT
$THETA  (0,.417)          ;3 V2 COEFFICIENT
$THETA  0.914             ;4 V2 EXPONENT
$THETA  (0,0.51)          ;5 V3 COEFFICIENT
$THETA  0.971             ;6 V3 EXPONENT
$THETA  (0,0.951)         ;7 Q  COEFFICIENT
$THETA  0.75              ;8 Q  EXPONENT
$THETA  (0,1.38)          ;9 CL WCK

$OMEGA BLOCK(4)
.0661
.001 .0979
.001 .001 .0338
.001 .001 .001 .0145

$SIGMA  .00854 .0446

$ESTIMATION     METHOD=1  INTERACTION  NOABORT  MAXEVAL=9000
                PRINT=15    SIGDIGITS=5  POSTHOC
```